

Truncated Life History Underlies Rapid Local Adaptation in Island Rattlesnake Venom Expression

Mark J. Margres ^{1,*}, Samuel R. Hirst ¹, Dylan G. Gallinson ¹, Rhett M. Rautsaw ¹, Preston J. McDonald ¹, Ella G. Guedouar ¹, Gunnar S. Nystrom ², Michael P. Hogan ^{2,3}, Schyler A. Ellsworth ², Kenneth P. Wray ⁴, Darin R. Rokyta ²

¹Department of Integrative Biology, University of South Florida, Tampa, FL 33620, USA

²Department of Biological Science, Florida State University, Tallahassee, FL 32306, USA

³Department of Ecology & Evolutionary Biology, University of Michigan, Ann Arbor, MI 48109, USA

⁴Biodiversity Center, University of Texas at Austin, Austin, TX 78703, USA

*Corresponding author: E-mail: margres@usf.edu.

Accepted: May 21, 2026

Abstract

Rapid adaptive evolution may be more likely to occur not only through standing genetic variation but via existing axes of genetic variation that have previously been exposed to selection. Ontogenetic variation represents one such axis and often evolves under strong selection in snake venoms. Snake venoms are complex cocktails of proteinaceous toxins, and ontogenetic shifts in venom expression are frequent and reflect dietary shifts across life history. Here, we used morphological, proteomic, transcriptomic, epigenomic, and optical genome mapping data to investigate a well-studied island-mainland population pair of eastern diamondback rattlesnakes (*Crotalus adamanteus*) to determine whether rapid adaptive expression divergence across populations occurred through the co-option of the ontogenetic regulatory network, population-specific changes independent of ontogeny, or a combination thereof. We found that island snakes were significantly smaller than mainland individuals, and venom proteomic data showed that the continuous ontogenetic shift in venom expression in the mainland population was truncated in island snakes. Venom-gland RNA-seq showed that island adults exhibited juvenile-like expression patterns at key transcription factors, and chromatin accessibility was predictive of venom gene differential expression for ontogenetically co-opted venom loci. Overall, rapid adaptation in the island population appears to have predominantly occurred through the co-option and truncation of the ontogenetic venom shift, with spatial differentiation playing a secondary role. Comparative tests in other systems are needed to determine whether rapid adaptation in general is not only biased toward standing genetic variation but toward large pre-existing axes of variation that have or continue to evolve under strong selection.

Key words: Ontogeny, chromatin accessibility, gene expression, structural variants, transcription factor.

© The Author(s) 2026. Published by Oxford University Press on behalf of Society for Molecular Biology and Evolution.

This is an Open Access article distributed under the terms of the Creative Commons Attribution-NonCommercial License (<https://creativecommons.org/licenses/by-nc/4.0/>), which permits non-commercial re-use, distribution, and reproduction in any medium, provided the original work is properly cited. For commercial re-use, please contact reprints@oup.com for reprints and translation rights for reprints. All other permissions can be obtained through our RightsLink service via the Permissions link on the article page on our site—for further information please contact journals.permissions@oup.com.

Significance

Identifying potential biases in how organisms rapidly adapt to novel environments is paramount for both predicting evolutionary responses and determining conservation management practices in the Anthropocene. Snake venoms evolve quite rapidly, and venomous snakes are often common on barrier islands, providing natural experiments in which to understand rapid, adaptive evolution. Here, we integrated multiple data types to investigate biases underlying rapid venom adaptation in a well-studied island population of eastern diamondback rattlesnakes. Ultimately, we found that rapid adaptation was biased toward the largest existing axis of venom expression variation (i.e. differences between adults and juveniles) across the range. As such, rapid adaptation in general may be biased not only toward standing genetic variation as previously proposed, but also toward existing axes of such variation that have evolved or continue to evolve under strong selection.

Introduction

Evolution can occur quite rapidly over ecological time-scales (Orr 2001; Carroll et al. 2007), and such rapid evolution is more likely to occur through standing genetic variation than *de novo* mutation (Barrett and Schluter 2007). Here, segregating beneficial alleles exist at higher frequencies and are immediately available to selection relative to *de novo* mutations (Innan and Kim 2004). Indeed, soft selective sweeps from standing genetic variation may be common (Messer and Petrov 2013), although their frequency in natural populations has been more recently questioned (Jensen 2014; Harris et al. 2018). Nevertheless, a perhaps underappreciated argument in favor of rapid adaptation through standing genetic variation is that, because such variation is present in the population, existing alleles may have already passed through a selective sieve in previous environments, distinct populations, and/or different age classes (Rieseberg et al. 2003; Barrett et al. 2008). As a result, we may expect the genetic mechanisms underlying rapid adaptation to be biased toward existing axes of genetic variation that presumably have or continue to evolve under strong selection.

One such axis may be ontogeny. Life history traits can evolve rapidly (e.g. Reznick et al. 2019), and because juvenile traits are subjected to selection earlier than adult phenotypes, selection on juveniles could ultimately affect traits expressed later in life (Donohue 2013). Indeed, evolutionary co-option of age class specific traits has led to adaptive evolution through, for example, pedomorphism (Voss and Shaffer 1997), and the added complexity of transitioning phenotypes may also provide more genetic source material (i.e. more standing genetic variation) upon which selection can act (Hogan et al. 2024). If the ecological selective pressures distinguishing age class also distinguish populations, we may expect ontogeny to preferentially contribute to within-species divergence.

Venoms have arisen independently >100 times among diverse animal lineages (Casewell et al. 2011;

Zancolli and Casewell 2020) and have been shown to exhibit extensive variation across life histories (Surm and Moran 2021). Snake venoms in particular have emerged as a model system for understanding the genetic basis of rapid adaptation (Margres et al. 2017; Schield et al. 2022; Nachtigall et al. 2025), and many snake species undergo ontogenetic shifts in venom expression (Mackessy 1988; Durban 2013; Hirst et al. 2024; Borja et al. 2025). Such shifts in venom expression likely reflect dietary shifts across life history (Mackessy et al. 2003); because snakes are gape-limited predators, head and body size ultimately constrain the maximum prey size a snake can consume (Shine 1991; Greene and Wiseman 2023). As a result, ontogenetic dietary shifts in snakes are quite common, with juveniles feeding on smaller prey and adults transitioning to larger prey (Forsman and Lindell 1993; Hampton 2018). Consequently, morphology and venom frequently evolve in parallel (Strickland et al. 2018; Schendel et al. 2019; Margres et al. 2021b; Xie et al. 2022), particularly across life history, including in the eastern diamondback rattlesnake (*Crotalus adamanteus*; Margres et al. 2015b).

Crotalus adamanteus is the largest rattlesnake species and native to the southeastern United States. *Crotalus adamanteus* has one of the best characterized venoms of any species (e.g. Margres et al. 2015a, 2016a, 2017), including a chromosome-level genome assembly with fully resolved venom-gene arrays (Hogan et al. 2024; Nachtigall et al. 2025), complete characterization of ontogenetic expression patterns of its venom genes (Margres et al. 2015b; Rokyta et al. 2017; Schonour et al. 2020), and recent identification of the *cis*- (CREs) and *trans*-regulatory elements (TREs) involved in its venom production (Hogan et al. 2024). The largest axis of variation in venom expression across the entire range of *C. adamanteus* is ontogeny, not population-level geographic differences, with juveniles expressing simpler venom phenotypes than adults (Margres et al. 2015b); such shifts appear to be fixed (Hogan et al. 2024). Adult and juvenile venoms have significantly different

functions (Margres et al. 2016b) and toxicities (Rokyta et al. 2017) associated with these expression differences, suggesting that the ontogenetic shift in venom expression is the product of selection in response to dietary changes. Indeed, *C. adamanteus* has been shown to largely consume mice (*Peromyscus* sp.) and cotton rats (*Sigmodon hispidus*) as juveniles with a significant shift toward larger prey items, notably rabbits, as adults (Means 2017). Different venom phenotypes have also been shown to co-vary with morphological traits associated with feeding (e.g. head size) in both ontogenetic and geographic contexts (Margres et al. 2015b). Therefore, we may expect that rapid, adaptive evolution in venom expression across *C. adamanteus* populations may be biased toward the co-option of the ontogenetic machinery through pedo- (i.e. retention of juvenile traits into adulthood) or peramorphosis (i.e. development beyond ancestral adult trait). Although we have several instances of putative venom pedomorphosis across (Mackessy et al. 2003; Calvete et al. 2010) and even within rattlesnake species (Hirst et al. 2026), we lack direct evidence of how the molecular machinery governing ontogenetic venom shifts provides the requisite substrate for rapid adaptive divergence within a single species.

Crotalus adamanteus frequently inhabits islands throughout its range (Means 2017), and islands have long provided natural experiments in which to investigate adaptive evolution (Losos et al. 1997; Millien 2006; Losos and Ricklefs 2009; Hirst et al. 2025). Previous work has established ontogenetic variation in (Guedouar et al. 2026) as well as rapid venom expression differentiation across several island populations of *C. adamanteus* (Margres et al. 2015a, 2016a, 2017), with the best characterized population on Little Saint George Island in north Florida (Fig. 1; Margres et al. 2017). Little Saint George Island lies ~7 km from the mouth of the Apalachicola River Delta in the Gulf of Mexico, and recent work estimates the island to be < 2,000 years old (Yao et al. 2022). Margres et al. (2017) showed that (1) both island and mainland *C. adamantus* populations were locally adapted to sympatric prey, with island venoms ~3× more toxic to island *S. hispidus* compared to mainland *S. hispidus*, and (2) island-mainland venom genes were significantly different in expression but not in sequence, demonstrating that rapid adaptation proceeded exclusively through expression differentiation. Yet the genetic mechanism(s) underlying these regulatory changes has yet to be investigated.

In general, gene expression can contribute to divergence in complex traits through copy number variation (Zhang et al. 2021), alteration of how the loci are regulated through CREs and TREs (Halfon 2017; Osada et al.

2017), and/or epigenetic modifications such as chromatin accessibility (Sackton et al. 2019). Here, we used proteomic, transcriptomic, epigenomic (ATAC-seq), and optical genome mapping data to determine if any of these mechanisms contributed to the previously described venom expression differentiation (Margres et al. 2017). Given that the epigenomic bases for age-related changes in *C. adamantus* venom expression have been previously characterized (Hogan et al. 2024), we ultimately sought to determine whether expression divergence across island-mainland *C. adamantus* populations occurred through the co-option of ontogeny, population-specific changes independent of ontogeny, or a combination thereof.

Results

Rapid Changes in Body Size in Island Rattlesnakes

Because body and head size are also critical traits that influence snake feeding ecology (Shine 1991; Margres et al. 2021c; Greene and Wiseman 2023), particularly in relation to ontogeny (Margres et al. 2015b), we first compared snout-vent length (SVL) for mainland ($n = 12$) and island ($n = 20$) adults (Table S1; Waldron et al. 2013; Margres et al. 2015b). We found that mainland adults were significantly larger than island adults ($p = 0.005$). Mainland snakes ($\mu = 117.375$ cm, $SD = 7.469$, $SE = 2.156$) were, on average, ~7 cm (i.e. ~6.5% of SVL) longer than their island counterparts ($\mu = 110.250$ cm, $SD = 6.845$, $SE = 1.531$); only two of the 20 island adults were > 120 cm SVL whereas seven of the 12 mainland adults were > 120 cm SVL (Fig. 2). To ensure these significant differences in size were not a result of detection biases in our field sampling approaches, we compared the mainland population to three other island sites sampled by the authors using identical methods (Margres et al. 2019): Sapelo and Jekyll Islands in Georgia, and Caladesi Island in Florida. We found that *C. adamantus* from Sapelo ($\mu = 129.255$ cm, $SD = 14.719$, $SE = 5.204$) and Caladesi ($\mu = 135.429$ cm, $SD = 21.759$, $SE = 8.224$) Islands were significantly larger, not smaller, than the focal mainland population from this study ($0.008 \leq p \leq 0.014$); Jekyll Island snakes were also larger ($\mu = 121.917$ cm, $SD = 14.297$, $SE = 4.127$) but not significantly so ($p = 0.170$). Collectively, these data showed that *C. adamantus* from Little St. George Island exhibited a significant and rapid reduction in body size.

Truncated Ontogenetic Venom Differentiation in Island Rattlesnakes

To test for significant venom expression differentiation across populations and age classes, we conducted a non-parametric MANOVA on venom protein expression data

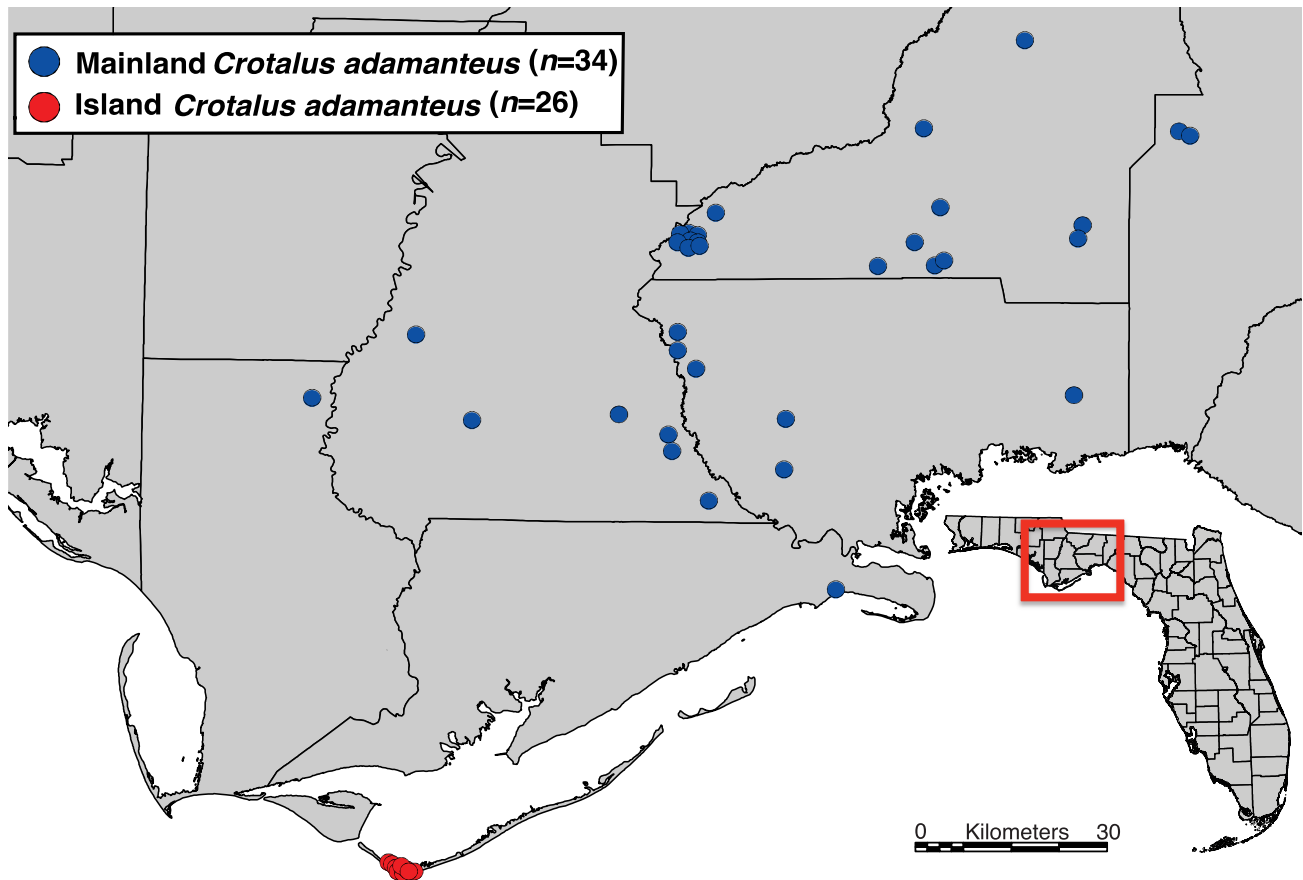


Fig. 1. Sampling of *Crotalus adamanteus*. We collected venom, tissues, and/or size data from 34 mainland and 26 island rattlesnakes. See [Table S1](#) for details.

for 46 individuals and detected significant expression differentiation across age classes ($p < 0.001$; $R^2 = 0.239$) and populations ($p = 0.007$; $R^2 = 0.054$; [Fig. 3a](#)). The interaction term between age class and population was also significant ($p = 0.034$; $R^2 = 0.037$), consistent with previous results across the entire range of *C. adamanteus* ([Margres et al. 2015b](#)); the significant interaction term suggested that differentiation across island and mainland snakes differed in degree between juveniles and adults. Therefore, we split the data set into four groups: island adults ($n = 17$), island juveniles ($n = 5$), mainland adults ($n = 9$), and mainland juveniles ($n = 15$). We re-conducted the non-parametric MANOVA and identified significant expression differentiation across groups ($p < 0.001$; $R^2 = 0.330$). All pairwise comparisons were significant following Bonferroni correction for multiple tests ($0.006 \leq p \leq 0.030$) except for the juvenile-juvenile comparison ($p = 0.504$; [Table 1](#)).

Ontogenetic expression variation, although significant in both island and mainland populations, was less pronounced in island snakes; ontogeny explained ~40% of

the variance in the mainland population but only ~14% of the variance in the island population ([Table 1](#)). We visualized group dispersions and found that island adult venoms were intermediate to mainland adult and both juvenile venoms ([Fig. 3b](#)); we confirmed this pattern by estimating group dissimilarity in venom expression (i.e. venom phenotypic distances between groups; [Table 1](#)) as previously described ([Margres et al. 2019](#)). We next performed a linear regression of principal coordinate 1 (PCoA1)~SVL to determine if size was explaining most of the variation in venom expression. We found a significant relationship for PCoA1~SVL ($p < 0.001$; $R^2 = 0.647$; [Fig. 3c](#)), suggesting that size differences were predictive of venom expression differentiation between island and mainland populations.

Venom-gland RNA-seq Identifies Patterns of Truncated Ontogeny and Spatial Differentiation in Venom Gene Expression

To identify the specific toxins underlying the significant venom expression differentiation described above, we

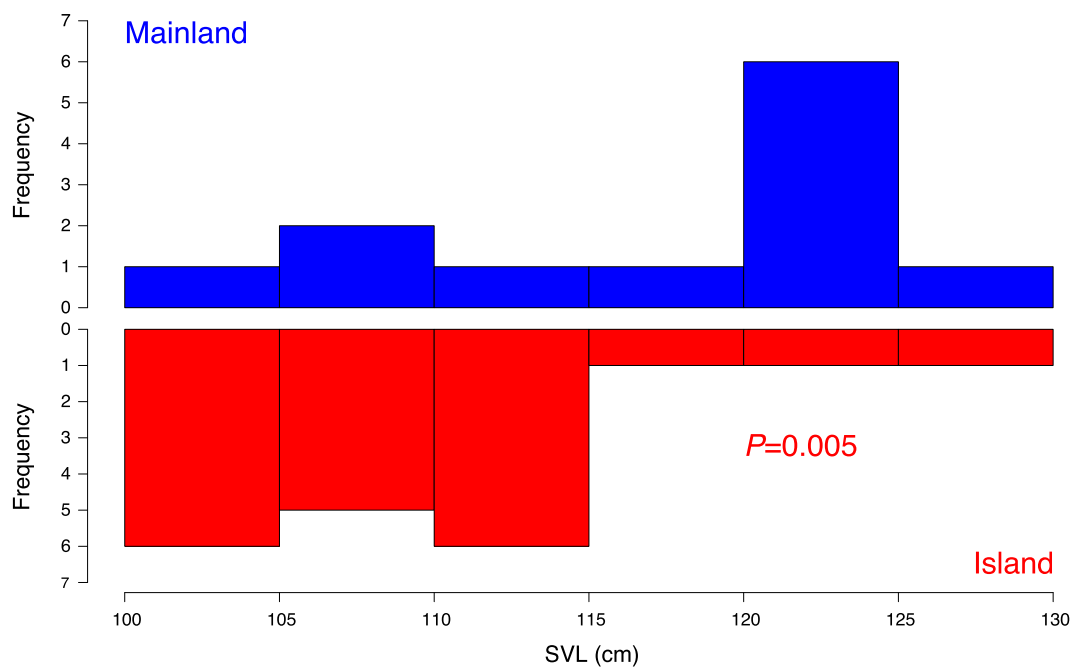


Fig. 2. Body size comparison for 12 mainland (upper blue) and 20 Little St. George Island (lower red) adult (≥ 1 m SVL) *Crotalus adamanteus*. Significance was established using a one-tailed *t*-test comparing snout-vent length (SVL).

used venom-gland transcriptomics to compare toxin gene expression across age classes and populations (Fig. 4, Fig. S1). Given our smaller sample sizes (mainland juvenile $n = 6$; mainland adult $n = 4$; island juvenile $n = 1$; island adult $n = 3$) relative to the proteomic analyses ($n = 46$), all toxins that exhibited a \log_2 fold change (LFC) > 1 were considered differentially expressed (DE). Note that we consider this smaller venom-gland RNA-seq data set as supplementary (albeit with greater, locus-specific resolution) to the larger, primary proteomic data set described above that established significant, truncated ontogenetic venom differentiation in the island population.

We found that island adults ($n = 3$) upregulated myotoxin (MYO) 5, β -defensin-03, and two snake venom serine proteases (SVSP-01, 08) relative to mainland adults ($n = 4$) whereas mainland adults upregulated six snake venom metalloproteinases (SVMPs) relative to island adults (Fig. 4a; Table S4). MYO-5 was also upregulated in mainland juveniles ($n = 6$) relative to mainland adults but was not DE between island adults and either juvenile population (Fig. 4a; Table S4), suggesting juvenile-like MYO-5 expression in island adults. Interestingly, despite only SVSP-01 and SVSP-08 exhibiting a LFC > 1 when comparing island and mainland adults, all 14 actively expressed SVSP paralogs were biased in expression toward island adults relative to mainland adults (Table S4).

Mainland adults upregulated only SVMPs relative to island adults (Fig. 4a), but not all 20 actively expressed

SVMPs were biased toward mainland adults (Table S4), differing from the patterns found in SVSPs. Here, SVMP-mad-3b was identified as DE in all four comparisons shown in Fig. 4a; SVMP-mad-3b was always biased toward adults (and mainland relative to island adults), supporting intermediate expression in island adults (Fig. 4a). Conversely, SVMP-mdc-3a was also biased toward mainland relative to island adults (Fig. 4a), yet Hogan et al. (2024) found that SVMP-mdc-3a was significantly biased toward juveniles across the range. We also found that SVMP-mdc-3a was significantly biased toward juveniles relative to adults in both populations (Fig. 4a, Fig. S4), suggesting spatial differentiation independent of the truncated ontogenetic shift.

Bradykinin-potentiating peptide (BPP-1), although not DE between island and mainland adults, showed intermediate expression in island adults ($\sim 7\%$) relative to mainland adults ($\sim 11\%$) and both juveniles where it was DE ($< 1\%$; Fig. 4b); mainland adult and juvenile BPP expression estimates were consistent with previous range-wide estimates for *C. adamanteus* (Hogan et al. 2024).

Transcription Factor Expression Correlates with Life History Truncation in Venoms

We found that island adults upregulated 124 transcription factors (TFs) and mainland adults upregulated 26 TFs relative to one another (LFC > 2 ; Fig. 4a; Table S4).

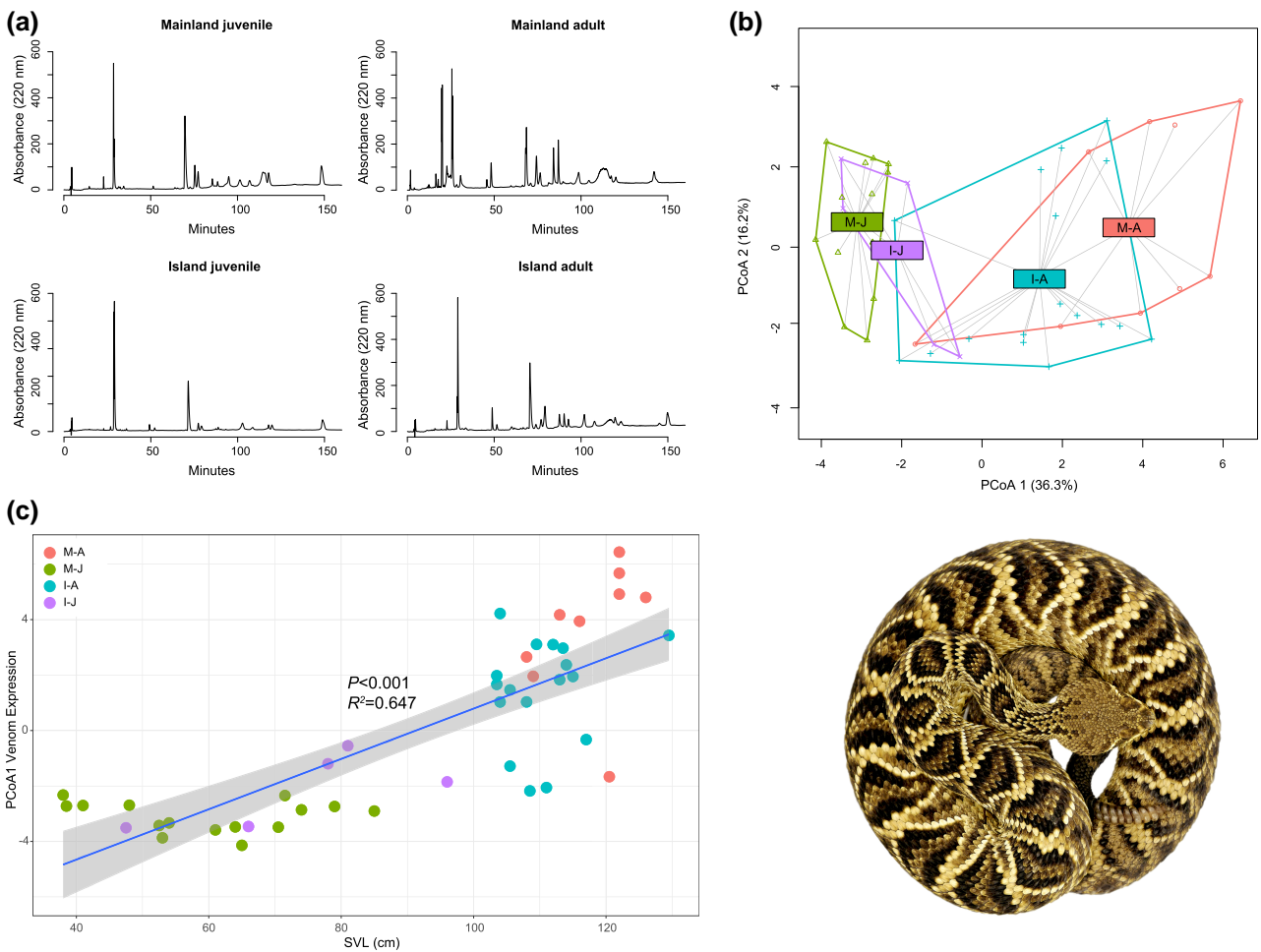


Fig. 3. Ontogenetic venom expression differentiation was truncated in island rattlesnakes. a) Reversed-phase high-performance liquid chromatography venom profiles for an adult and juvenile from each population. Peaks represent toxins, and the area under each peak represents toxin abundance. b) A group dispersion plot of venom expression for age class × population. Labels occur at the cluster centroid, line segments connect group members to centroid, and axes are principal coordinates. c) A linear regression of PCoA1 from panel B and SVL revealed a significant relationship ($p < 0.001$), indicating size was explaining most of the variation in venom expression across groups. Gray shading indicates confidence limits, and colors correspond to panel B. Abbreviations: I-A, island adult; I-J, island juvenile; M-A, mainland adult; M-J, mainland juvenile; SVL, snout-vent length. Photo credit: M. Hogan.

Table 1. Pairwise comparisons of venom differentiation across age class × population.

	Mainland Adult (MA)	Mainland Juvenile (MJ)	Island Adult (IA)	Island Juvenile (IJ)
MA	X	$p = 0.006$; $R^2 = 0.403$	$p = 0.030$; $R^2 = 0.117$	$p = 0.012$; $R^2 = 0.299$
MJ	8.990	X	$p = 0.006$; $R^2 = 0.278$	$p = 0.504$; $R^2 = 0.082$
IA	7.326	7.430	X	$p = 0.012$; $R^2 = 0.142$
IJ	8.700	5.680	7.170	X

Values above the diagonal represent results of pairwise non-parametric MANOVAs; all p -values were Bonferroni-adjusted. Values below the diagonal represent Euclidean distances between groups (i.e. group dissimilarity).

Gene ontology (GO) analyses yielded a single significant result and identified that island adult-biased TFs were significantly enriched (adjusted p -value and q -value < 0.001) for DNA binding (GO:0003677); mainland

adult-biased TFs were not significantly enriched for any GO category.

Given that the GO results were limited in scope, we looked at specific candidate TFs that were DE across

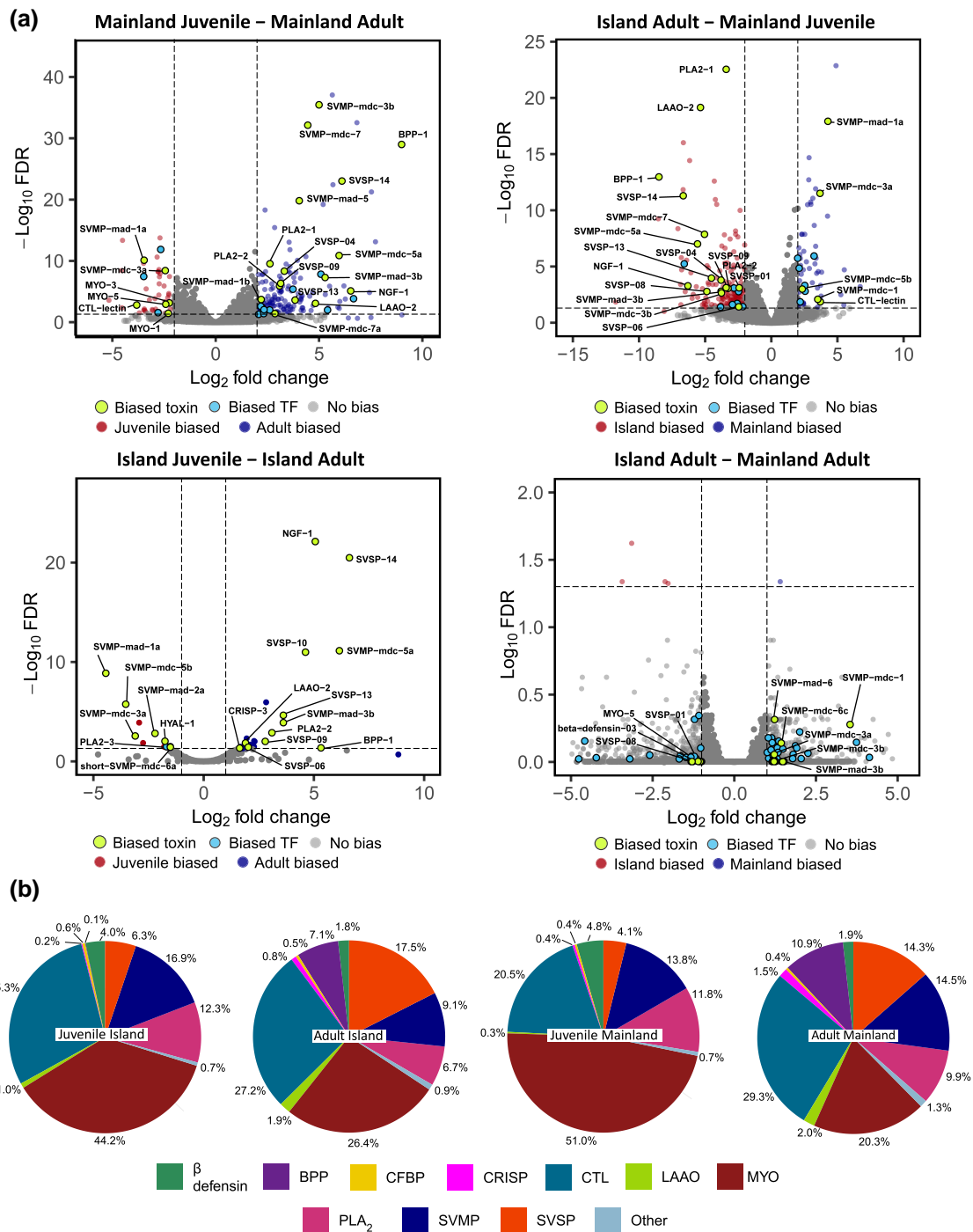


Fig. 4. Venom-gland transcriptomics shows expression differences across island and mainland adults exhibited both spatial and ontogenetic divergence patterns. a) Volcano plots depicting venom gland differential expression across mainland juveniles ($n = 6$) and adults ($n = 4$), mainland juveniles and island adults ($n = 3$), island juveniles ($n = 1$) and adults, and island and mainland adults. Toxins with a \log_2 fold change > 1 and FDR-adjusted p value (FDR) < 0.05 were considered biased (highlighted in green). For the comparison between island and mainland adults, toxins were shown as biased if \log_2 fold change > 1 regardless of FDR. b) Pie charts showing mean transcripts per million (TPM) per toxin class for juveniles and adults for each population. Abbreviations: BPP—Bradykinin-potentiating peptide, CFBP—Snaclec coagulation factor IX-binding protein, CRISP—Cysteine-rich secretory protein, CTL—C-type lectin, LAAO—L-amino acid oxidase, MYO—Myotoxin, PLA₂—Phospholipase A₂, SVMP—Snake venom metalloproteinase, SVSP—Snake venom serine protease, TF—Transcription factor.

Table 2. Differentially expressed candidate ontogenetic transcription factors.

TF	Expression bias this study	Expression bias Hogan et al. (2024)	Consistent with co-option
Lhx6	Island adult	Juvenile	Yes
Nfil3	Mainland adult	Juvenile	Yes (see Discussion)
Fosl2	Mainland adult	Adult	Yes
Csrnp1	Mainland adult	Adult	Yes
Fosb	Mainland adult	Adult	Yes
Nr4a3	Mainland adult	Adult	Yes

Abbreviations: TF - transcription factor.

island and mainland adults. Island adults upregulated several Hox paralogs (i.e. four of the top 12 DE TFs including the top two most DE TFs; Table S2). In total, 13 Hox paralogs were DE, with 12 biased toward island adults and only one upregulated in mainland adults. Specifically, *Hoxa5* was upregulated in island adult snakes, and the overexpression of this specific paralog in mice has previously been linked to dwarfism (see Discussion; Foucher et al. 2002).

Of the > 1 k putative TFs expressed in *C. adamanteus* venom glands, Hogan et al. (2024) found that 37 TFs were DE across age classes range-wide. Of these 37 candidate ontogenetic TFs, six were identified as DE in our data set (Table 2). *Lhx6* was the only candidate TF biased toward island adults whereas five other candidate TFs were biased toward mainland adults. The expression of all six TFs was consistent with life history truncation, with juvenile-biased TFs being up-regulated in island adults and adult-biased TFs being up-regulated in mainland adults (Table 2).

Differential Chromatin Accessibility Predicts Differential Expression Across Populations

We analyzed venom-gland ATAC-seq data (mainland adults: $n = 2$; island adults: $n = 2$) to test for differential accessibility (DA) in and near DE venom genes. We first tested for an overall association between venom gene expression and epigenetic patterns as previously described (Hogan et al. 2024). DA ATAC-seq peaks (Table S5) exhibited a significant positive correlation with DE venom genes for peaks within venom genes ($p < 0.001$; $R^2 = 0.170$) as well as within 1 kb ($p = 0.035$; $R^2 = 0.111$) and 10 kb ($p < 0.001$; $R^2 = 0.540$) of venom genes (Fig. S2B); results were robust to multiple filtering strategies as well as the inclusion of outliers (Figs. S2, S3).

To identify DA venom genes across island and mainland adults, we required concordant $LFC \geq 1$ across more than one filter and found seven island adult-biased and seven mainland adult-biased DA venom genes (Fig. 5;

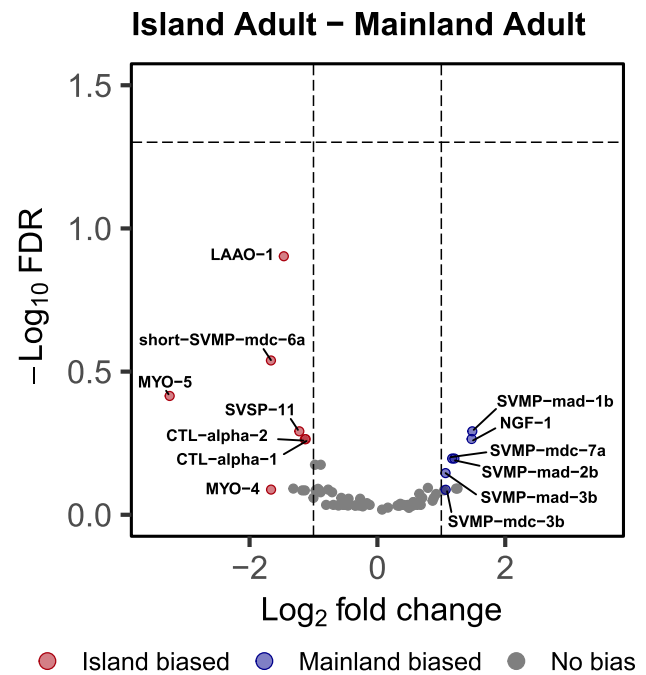


Fig. 5. Venom-gland ATAC-seq shows differential chromatin accessibility across island and mainland adults is concordant with differential expression. Volcano plot depicting venom gland differential chromatin accessibility across mainland ($n = 2$) and island ($n = 2$) adults. \log_2 fold change (LFC) and FDR-adjusted p values (FDR) were calculated as the median across the four HTSeq-count filtering schemes (see Materials and Methods). Toxins with a LFC > 1 in at least two HTSeq-count filtering schemes (regardless of FDR) were considered biased (highlighted in red and blue, respectively). Note that genes with LFC > 1 which are not indicated as being biased in the plot exhibited LFC > 1 under only a single filtering scheme. For each gene, the region (10kb flank, 1kb flank, or genic) with the greatest LFC is shown. Toxin gene β -defensin-3 (mainland biased; LFC = 4.03; $-\log_{10}$ FDR = 7.00) was omitted from the plot for visualization purposes; see Fig. S4. Abbreviations: CTL—C-type lectin, LAAO—L-amino acid oxidase, MYO—Myotoxin, SVMP—Snake venom metalloproteinase, SVSP—Snake venom serine protease.

Table S5); these accessibility differences were largely concordant with the expression differences described above. For example, although MYO-5 was the only island-biased DA venom gene that also exhibited island-biased DE with a LFC > 1, all seven island-biased DA venom genes were more highly expressed in island than mainland adults. Of the seven mainland-biased DA venom genes, SVMP-mad-3b, SVMP-mdc-3b, and SVMP-mdc-6c exhibited mainland-biased DE with a LFC > 1; SVMP-mad-1b also showed mainland-biased expression (LFC < 1). The other three loci, however, showed island-biased expression despite mainland-based DA; β -defensin-03 exhibited island-biased DE with a LFC > 1, and both SVMP-mad-2b and SVMP-mdc-7a showed island-biased expression

(LFC < 1). These putatively discordant signals may be caused by the genomic organization of these venom genes in large tandem arrays (see Discussion). Given that these gene-specific DA results were significantly more concordant with the DE results than expected by chance (χ^2 $p = 0.034$), however, chromatin accessibility clearly, at least in part, predicted adaptive differential venom expression across populations.

Putative Regulatory Variants in Chromatin Accessible Genomic Regions May Contribute to Expression Variation Independent of Ontogeny

We next explored sequence variation in ATAC-seq peaks within and flanking venom genes across island ($n = 2$) and mainland ($n = 6$) snakes to identify putative variants associated with venom DE. Because of our small sample sizes, we focused on fixed differences and unique alleles in the island population; note here that we also included mainland juveniles in the analyses (see Materials and Methods).

We identified a single fixed difference for *Vespryn-1*. *Vespryn-1* did exhibit mainland adult-biased DA under one filter and was more highly expressed in mainland relative to island adults, although not significantly so (LFC < 1). We also identified 12 unique alleles in the island population: four alleles also associated with *Vespryn-1*, one allele each for *Kun-1*, *CTL-snaclec-subunit-gamma-1*, *CTL-snaclec-subunit-beta-3*, and *SVSP-15*, and two alleles each for *SVMP-mdc-1* and *SVSP-16*. *Kun-1*, *CTL-snaclec-subunit-gamma-1*, and *CTL-snaclec-subunit-beta-3* were not DE or DA between island and mainland adults, suggesting these variants may not have a regulatory effect or affect the regulation of other genes. *SVMP-mdc-1*, however, was DE (LFC > 3.5) and biased toward mainland adults (Fig. 4a; Table S4). Additionally, although neither *SVSP-15* or *SVSP-16* were individually identified as DE or DA, the entire *SVSP* gene family exhibited greater expression levels in island than mainland adults as stated above (Table S4).

Structural Variants in Large Venom Gene Families May Contribute to Venom Differentiation Independent of Co-option

Lastly, because structural variants (SVs) can affect gene expression independent of life history (i.e. genes are not duplicated or deleted within the same genome as an animal ages), we used the Bionano optical genome mapping rare-variant analysis (RVA) pipeline to identify large SVs in a single island animal relative to the publicly available mainland reference genome (Hogan et al. 2024); evidence of SVs altering venom regions that were DE would support spatial differentiation independent of life history rather than co-option. We identified 18,907 total SVs that passed filters: 10,510

deletions, 8,105 insertions, 63 duplications, 166 inversions, 48 interchromosomal translocations, and 15 intrachromosomal duplications (Table S6). Of these, 33 SVs overlapped genomic regions containing venom genes: 29 deletions, two duplications, and two inversions. Most major venom gene families displayed evidence of deletion and duplication events between mainland and island populations, including the three most DE venom gene families (*SVSP*, *SVMP*, and *MYO*).

In particular, we found evidence for two specific SVs that may contribute directly to the venom DE described above. First, the RVA analysis detected a substantial number of overlapping deletion, duplication, and inversion events in the *MYO* region of chromosome 2, indicating a complex and dynamic genomic architecture, consistent with previous work in this system (Margres et al. 2017). Second, a deletion event was identified in an intergenic region between *SVMP-mdc-1a* and *SVMP-mdc-3a*. Both loci were more highly expressed in mainland than island adults (*SVMP-mdc-3a* with a LFC > 1), and the deletion overlapped an accessible ATAC-seq peak present in all sequenced adults ($n = 4$).

Discussion

Rapid Changes in Body in Response to Putative Dietary Shifts in Island Rattlesnakes

We found that island adults were significantly smaller than their mainland counterparts (Fig. 2). Changes in body size following island colonization is a common phenomena (Foster 1964; Van Valen 1973). Larger species often become dwarfed, and smaller species often exhibit gigantism due to changes in resource availability, competition, predation, and/or other ecological factors and developmental constraints (Lomolino 2005). Although snakes have been shown to exhibit examples of both insular dwarfism and gigantism (Iverson 1986; Boback and Guyer 2003; Lillywhite and Martins 2019; Vanek and Burke 2020), the predictability of such changes in snakes appears reduced relative to mammals. Such equivocal results have been proposed to be the result of food availability/quality playing a larger role in snakes (Forsman 1991; Keogh et al. 2005). The optimal body size for any island population is at least partially, if not predominantly, a product of food availability (Case 1978), with reductions in size being the product of food scarcity and increases in body size being the product of food abundance. Indeed, congener *C. oreganus* has been shown to exhibit dwarfism on Anaho Island in Pyramid Lake in Nevada (Keehn et al. 2013), and such reductions in body size were predicted to be the result of dietary changes from mammals to lizards; small mammals have been shown to have greater

nutritional value than lizards (Zuffi et al. 2010), supporting resource quality as an important metric in determining insular snake size.

Crotalus adamanteus is a small mammal specialist (Means 2017). Previous trapping by the authors revealed that *S. hispidus* was largely the only available prey source on Little St. George Island (except for a few gray squirrels [*Sciurus carolinensis*] limited to the immediate vicinity of an old homestead) whereas multiple prey species, including larger prey items such as rabbits (*Sylvilagus* sp.) and woodrats (*Neotoma* sp.), were available on the mainland (Margres et al. 2017; Means 2017). Schonour et al. (2020) summarized the data of Means (2017) and showed that mainland snakes exclusively consumed mice (*Peromyscus* sp.) and *S. hispidus* at smaller sizes (i.e. <80 cm) with a significant shift toward larger prey items, notably rabbits, once the snakes exceeded 132 cm SVL. Of the 20 adults collected from Little St. George Island, none exceeded 132 cm SVL (Fig. 2), perhaps, at least partially, because rabbits were not available. Rabbits have been documented to occur on the other three islands where *C. adamanteus* were larger than the focal mainland population (pers. obs. M.J.M). Rabbit presence-absence and, therefore, prey size/quality may play an important role in determining insular *C. adamanteus* body size, consistent with other venomous snake populations (Forsman 1991; Keogh et al. 2005).

Whether the significant size reduction in island snakes was a heritable change in body size due to selection (i.e. evolution) or environmentally-induced (i.e. plasticity) because of differences in resource availability was unclear with the current data. Indeed, the data were consistent with both plasticity in body size driven by changes in prey quality as well as local adaptation for different body size optima across populations. Distinguishing between these different processes would require common garden experiments that were beyond the scope of the current study; we discuss this in more detail below. Additionally, we note that size dimorphism does exist among most rattlesnake species (e.g. Gibbons 1972), and the population differences in body size could result from differences in sex ratios among the sampled individuals. Unfortunately, we did not possess sex information for enough individuals to perform a statistical analysis; as a result, we cannot eliminate sex bias as a confounding variable underlying differences in population body size, although we have no reason to believe such a bias would exist in our data.

Co-option of Ontogenetic Venom Expression Underlies Rapid Adaptation in Island Rattlesnakes

We found significant venom protein expression differentiation across age classes and populations (Fig. 3),

consistent with previous work (Margres et al. 2017). The expression patterns here, however, showed for the first time that the continuous ontogenetic venom shift in the mainland population (Schonour et al. 2020) was truncated in the island population. Schonour et al. (2020) argued that dietary shifts in venomous snakes should predict the tempo of ontogenetic variation in venom expression. Given that island snakes never attained sizes where mainland snakes were switching to rabbits (Means 2017), truncation of life history as evidenced through suspended venom ontogeny would likely be advantageous. Indeed, previous work showed that island adult venoms were $\sim 3\times$ more toxic to island *S. hispidus* than to mainland *S. hispidus* (Margres et al. 2017), indicating the venom expression differences described here were adaptive. Our results suggested that altered predator-prey interactions in the island population underlay the rapid morphological and venom expression divergence evident between mainland and island adult snakes.

Although life history was truncated regarding island venom expression, this was not an example of true pedomorphism as island snakes still exhibited a significant ($p = 0.012$), albeit reduced ($R^2 = 0.142$), ontogenetic shift in venom expression relative to the mainland population ($R^2 = 0.403$). Although whether changes in body size were the result of plasticity or distinct genotypes across populations was unknown as discussed above, prior work in *C. adamanteus* (Margres et al. 2015b) and other rattlesnakes (Gibbs et al. 2009) has shown venom expression to not be plastic. With that said, ultimately confirming that venom expression divergence was the result of evolutionary change rather than plasticity would require translocation experiments to determine if island snakes would reach larger sizes and achieve the terminal adult venom phenotype on the mainland (and vice versa); such experiments are not currently possible. Regardless, we collectively showed here and elsewhere (Margres et al. 2017) that the truncation of the ontogenetic venom shift in the island population significantly increased toxicity to island prey and was, therefore, adaptive.

RNA-seq Identifies Evidence of Both Life History Co-option and Independent Spatial Differentiation in Venom Expression

Although our proteomic data indicated a clear truncation of the ontogenetic venom shift at the trait-level as described above, the resolution of these data prevented the identification of specific DE loci and, therefore, comparisons to previous characterizations of range-wide ontogenetic venom expression patterns (Hogan et al. 2024). We used venom-gland RNA seq to

explore locus-specific signals of ontogenetic co-option and spatial differentiation independent of ontogeny and found evidence of each in island snakes. For example, island adults exhibited juvenile-like MYO-5 expression, consistent with the truncation of the ontogenetic shift. Similarly, BPP-1 showed intermediate expression in island adults relative to mainland adults and both juveniles. Hogan et al. (2024) found that BPP upregulation in adults corresponded to the largest gene family-level ontogenetic expression change across all toxin genes, with range-wide mean BPP adult expression of ~16%. Yet we found that upregulation to be truncated in island adults relative to their mainland counterparts (Fig. 4b) as well as range-wide (Hogan et al. 2024), supporting truncated ontogenetic venom differentiation in the island population. Island adults, however, also showed an up-regulation of the entire SVSP gene family which was not associated with ontogeny; juvenile venoms were characterized by reduced SVSP expression relative to adult venoms in both populations (Fig. 4b). All 14 actively expressed SVSP paralogs were biased in expression toward island adults relative to mainland adults (Table S4); such consistent expression suggested either concordant regulatory evolution across the entire gene family or that paralog sequence similarity prevented unique read mapping. The 14 expressed SVSP paralogs exhibited substantial sequence divergence, however, with 91 unique comparisons yielding a mean pairwise identity of 81.47%, ranging from 65.30%–98.60%, suggesting complete biased expression of the SVSP gene family toward island adult snakes. Conversely, mainland adults were characterized by an up-regulation of SVMPs. While SVSPs exhibited concordant, gene-family wide changes supporting spatial differentiation independent of ontogeny, the SVMP gene family exhibited paralog-specific expression changes indicative of both life history truncation (e.g. SVMP-mad-3b) and spatial differentiation (e.g. SVMP-mdc-3a). Although the expression of SVMP-mdc-3a was not consistent with ontogenetic co-option (Hogan et al. 2024), the downregulation of SVMPs in island adults was consistent with a truncated life history. SVMPs have long been proposed to aid in prey digestion given the tissue necrosis and damage their activities cause (Mackesy 1988, 2010) and may not be required to effectively digest smaller prey (Margres et al. 2015b). Given that smaller rodents are the only available prey on Little St. George Island, the down-regulation of these six SVMPs in island adults was consistent with the life history changes described above.

Pedomorphic-like TF Expression in Island Adult Snakes Likely Contributed to Truncated Venom Ontogeny

We found clear evidence of pedomorphic-like expression in island adult snakes at key, previously described

candidate TFs (Table 2; Hogan et al. 2024). Lhx6 was the only candidate TF biased toward island adults whereas Nfil3, Fosl2, Csrnp1, Fosb, and Nr4a3 were biased toward mainland adults. Lhx6 was classified as juvenile-biased by Hogan et al. (2024), consistent with our adult-juvenile comparisons across both island and mainland populations and, therefore, life history truncation. Four of the five mainland-biased candidate TFs were biased toward adults in Hogan et al. (2024); the only exception was Nfil3 which was upregulated in mainland adults here but juvenile-biased range-wide. Nfil3 was, however, adult-biased in our study when comparing mainland adults and juveniles (and not DE across island adults and juveniles), indicating (1) geographic variation in the contributions of TFs to ontogenetic shifts across the range, and (2) consistency with life history truncation. Overall, these patterns support pedomorphic-like TF expression in island adult snakes that likely contributed to truncated venom ontogeny.

We also found a number of Hox genes that were island adult-biased in expression. Hox genes are master regulators of animal development (Krumlauf 1994; Mallo and Alonso 2013), including in reptiles (Martín-del Campo et al. 2019) and specifically snakes (Di-Poi et al. 2010; Head and Polly 2015). Although Hox genes are often the focus of studies on embryonic development (e.g. limb formation and body plan variation; reviewed in Mallo 2018), their expression and functional roles may often persist into adulthood (Rux and Wellik 2017). Here, we found that Hoxa5 was upregulated in island adult snakes, and the overexpression of this specific paralog in mice has previously been linked to dwarfism (Foucher et al. 2002). Hoxa5 was DE and biased toward island adults in all comparisons but was not DE in any comparison excluding island adults (Table S2), suggesting this particular TF may be contributing to life history truncation and/or changes in body size. Future functional work validating the role of this TF in snakes and specifically its expression in venom glands relative to other tissues is required to further explore any broader relationship with body size variation.

Given the timescale of divergence in island snakes (i.e. <2,000 years Yao et al. 2022), simple, singular molecular switches may be enabling rapid ontogenetically-biased expression changes in the venom phenotype; such switches would highlight how the genetic architecture of the venom system (i.e. tandem arrays) may allow few molecular changes to cause large phenotypic effects over very short timescales. TFs may provide such a mechanism.

Differential Chromatin Accessibility Contributes to Differential Venom Expression Across Populations

We found that chromatin accessibility predicted adaptive differential venom expression across populations, consistent with prior work in venoms (Margres et al.

2021a; Perry et al. 2022; Gopalan et al. 2024; Hogan et al. 2024) and other systems (Lewis and Reed 2018; Xin et al. 2020). As described above, Hogan et al. (2024) showed that DA played a deterministic role in *C. adamanteus* venom ontogeny. Here, we showed that DA predicted DE for venom genes associated with both truncation of the ontogenetic shift (e.g. MYO-5, SVMP-mad-3b, SVMP-mdc-6c) as well as spatial differentiation independent of ontogeny (e.g. SVMP-mdc-3a, SVSP-11). Chromatin accessibility, therefore, appears capable of playing a major role in governing adaptive venom expression differences over ontogeny (Hogan et al. 2024), through the co-option of ontogeny across populations, as well as across populations independent of ontogeny (at least in *C. adamanteus*) over exceptionally short timescales. As ATAC-seq and other techniques become more accessible in non-models (Erdoğan et al. 2025), we may come to realize that DA and other epigenomic mechanisms play a much larger role in rapid, adaptive evolution than previously understood.

We do note, however, that several loci (e.g. SVMP-mad-2b) exhibited putatively discordant DA-DE signals that may be the result of venom genomic architecture. SVMPs and other venom gene families occur in large tandem arrays in rattlesnakes (Schield et al. 2019; Margres et al. 2021a; Hirst et al. 2024; Hogan et al. 2024); here, a peak we associated with one paralog based on linear distance may actually contribute to the regulation of a different paralog in the array. Hogan et al. (2024) found broader regions of accessibility and higher densities of TF-binding motifs near large venom-gene arrays in comparison to non-venom genomic regions, and three-dimensional proximity has been shown to provide more robust regulatory element associations than linear proximity (Schoenfelder et al. 2018). Both MYOs (including β -defensins) and SVMPs occur in large tandem arrays in the *C. adamanteus* genome (Hogan et al. 2024; Nachtigall et al. 2025), suggesting this putative discordance was likely the result of paralog misassignment rather than DA not explaining DE. Future work incorporating techniques such as Hi-C Coupled chromatin cleavage and Tagmentation (HiCuT; Sati et al. 2022) will be necessary to assign regulatory elements such as enhancers to specific target genes and resolve such discordance.

Putative Regulatory Variants in Chromatin Accessible Genomic Regions May Contribute to Expression Variation Independent of Ontogeny

Given that (1) regulatory variants have been shown to exhibit significant enrichment in promoters and enhancers (Wang et al. 2013; Das et al. 2015; Wen et al. 2016; GTEx Consortium 2017), and (2) > 75% of chromatin

accessible regions represent enhancers and promoters (Yan et al. 2020), we explored sequence variation in ATAC-seq peaks within and flanking venom genes across populations. Despite small sample sizes, we identified several putative regulatory variants that may contribute to venom expression variation across populations. As expected, the top three candidate SNPs all occurred in/near venom genes not associated with ontogenetic co-option (SVMP-mdc-1, SVSP-15, 16). Because selection on ontogenetic traits is constrained to act on a singular genome (Kawajiri et al. 2014), ontogenetic trait variation is limited to age-specific expression variation. We, therefore, did not expect allelic variation in putative regulatory regions to contribute to ontogenetic co-option. Here, our results instead suggest evidence of geographically-variable selection on putative regulatory variants altering expression of specific venom loci independent of ontogenetic co-option. Ultimately, larger sample sizes and functional genomic work are needed to further explore the role of these putative candidate alleles, and additional demographic models could explore the relationship between local adaptation and gene flow. Prior work in the system explored migration rates between island and mainland populations using > 250 loci and > 420 k sites (Margres et al. 2017) and found that panmixia was the best model under a coalescent framework (Beerli 2008), indicating either (a) the rapidity of adaptation and the lack of time for neutral differentiation to occur in the absence of gene flow, or (b) adaptation in the face of gene flow. Additional SNP data are needed to disentangle these hypotheses and further evaluate the variation in putative CREs identified here in the context of migration-selection balance.

Structural Variants in Venom Tandem Arrays Likely Contribute to Venom Differentiation Independent of Ontogenetic Co-option

We used Bionano optical genome mapping and identified thousands of SVs across one island and one mainland adult (Table S6), including evidence for two specific SVs that potentially contributed to the venom DE across populations. First, we identified multiple overlapping SVs in the MYO region of chromosome 2. Prior work showed that MYO SVs were common across the range of *C. adamanteus*, including in these two populations (Margres et al. 2017), and MYO variability is not unique to *C. adamanteus* (Cameron and Tu 1978; Strickland et al. 2018; Smith et al. 2023) and may be linked to its mammal-specific toxicity (Mackessy and Saviola 2016). The data here provide additional evidence and support for extensive variation in the region, but the exact structure of the rearrangement was too

complex to resolve with the Bionano optical genome mapping data ($n = 1$) alone. Long-read sequencing data for multiple individuals for each population could likely resolve the structure of the rearrangement, but such data were outside the scope of the current study.

Second, we found a deletion in an intergenic region between two mainland-biased DE SVMPs (SVMP-mad-1a, SVMP-mdc-3a). Importantly, the deletion overlapped an accessible ATAC-seq peak present in all sequenced adults ($n = 4$), suggesting a deletion of a putative regulatory element. The deletion of a CRE governing the expression of these DE venom genes would certainly impact expression, but additional techniques (e.g. HiCuT) and larger sample sizes would again be necessary to assign CREs to their target genes; we again leave this for future work.

Similar to allelic variation in putative regulatory regions, we did not expect SVs to contribute to ontogenetic co-option but only spatial differentiation independent of life history. Although the DE and DA of MYOs was consistent with ontogenetic co-option as described above, the unresolved yet clear, significant signal of SVs in that region suggest that multiple mechanisms may enable rapid, adaptive expression differentiation within a single gene family. Conversely, as mentioned above, the DE of SVMP-mdc-3a was indicative of geographically-variable selection independent of the truncated ontogenetic shift, indicating that SVs, particularly in this gene family (Nachtigall et al. 2025), can occur over very short timescales and contribute to rapid adaptation. Given that these analyses were limited by only comparing one individual from each population, additional SVs in venom regions may be frequent (but not fixed) in either population and affect venom function; additional data and approaches (e.g. pangenomes; Fang and Edwards 2024) are needed to comprehensively address the role of SVs in population divergence.

Conclusion

We sought to determine whether rapid, adaptive expression divergence across island-mainland *C. adamanteus* populations occurred through the co-option of ontogeny, population-specific changes independent of ontogeny, or a combination thereof. Overall, rapid adaptation in the island population appears to have predominantly occurred through the co-option of the ontogenetic venom shift, the largest axis of venom variation in the species (Margres et al. 2015b), with spatial differentiation playing an important but secondary role. Venom proteomic expression data strongly indicated ontogenetic co-option, yet higher resolution venom-gland RNA-seq data provided evidence of both co-option and population-specific changes independent of ontogeny at the individual gene level.

Interestingly, the same RNA-seq data showed that TF expression was unequivocally supportive of co-option as island adults exhibited juvenile-like TF expression patterns. Epigenomic data showed that chromatin accessibility was predictive of DE regardless of whether co-option was involved, suggesting that both ontogenetic and population-specific expression patterns may be mediated by chromatin accessibility. Together, our data suggest that rapid adaptation across populations occurred through the co-option and truncation of the venom ontogeny regulatory network mediated by TF expression. We may therefore expect that rapid adaptation in other systems to not only be biased toward standing genetic variation (Barrett et al. 2008) but perhaps existing axes of variation that have already been exposed to selection (Rieseberg et al. 2003), especially if those axes of variation are regulated by key TFs.

Materials and Methods

Sampling

We collected venom, tissues, and/or size information from 34 mainland ($n = 13$ adults, $n = 21$ juveniles) and 27 island ($n = 22$ adults, $n = 5$ juveniles) *C. adamanteus* (Table S1). Age class assignment was based on length (i.e. adults ≥ 1 m SVL) as previously described (Waldron et al. 2013; Margres et al. 2015b). Island *C. adamanteus* were collected from Little St. George Island, and mainland *C. adamanteus* were collected from the adjacent mainland region as previously described (Margres et al. 2017). All samples were collected under Florida Fish and Wildlife Conservation Commission permits LSSC-13-00004, LSSC-09-0399, LSSC-12-00071A, and LSSC-20-00037A. All animal procedures were approved by the Institutional Animal Care and Use Committees (IACUC) at Florida State University (#0924, #1333) and the University of South Florida (IS00008815, IS00009536). Table S1 indicates which individuals were included in each analysis described below.

Testing for Differences in Body Size

To determine whether island snakes were significantly smaller than mainland snakes, we used a one-tailed *t*-test to compare SVL for 12 mainland and 20 island *C. adamanteus* that were ≥ 1 m SVL. Previous work has shown that *C. adamanteus* reaches sexual maturity at ~ 1 m SVL (Waldron et al. 2013), and ontogenetic shifts in venom expression also occur near this threshold (Margres et al. 2015b; Schonour et al. 2020; Hogan et al. 2024). We restricted our analyses to adults to account for known sampling biases across age classes and populations. For example, many more juvenile

snakes (i.e. <1 m SVL) were collected from the mainland population, and including these individuals in the analysis would have biased the mainland population toward a smaller mean size. Analyses were also restricted to wild-caught adults with size information at time of capture (Table S1). To ensure comparisons across Little St. George Island and the adjacent mainland region were not biased by differences in field sampling methods (e.g. predominantly driving roadways on the mainland versus hiking suitable habitat on the island), we compared the mainland population to three other island sites sampled by the authors using identical methods from a previous study (Margres et al. 2019): Sapelo and Jekyll Islands in Georgia, and Caladesi Island in Florida. All metadata associated with those individuals can be found in Margres et al. (2019).

Estimating Venom Protein Expression Differentiation

To characterize venom protein expression for all samples, we quantified 25 reverse-phase high-performance liquid chromatography (RP-HPLC) peaks for each venom sample as previously described (Margres et al. 2014, 2017). Raw data are in Table S2. To test for significant expression differentiation across populations and age classes, we followed the statistical approach of Margres et al. (2015a, 2017). Briefly, we first used a multiplicative replacement strategy (Martin-Fernandez et al. 2003) assuming a detecting threshold of 0.01% to remove zeros from the raw data. We next used the isometric log-ratio (ilr) transformation (Egozcue et al. 2003) to transform the data using the `robCompositions` package (Templ et al. 2011) in R. To test for significant expression differentiation across groups, we performed a non-parametric MANOVA using the `adonis` function from the `vegan` package (Oksanen et al. 2013) in R on the ilr-transformed data using Euclidean distances as previously described (Margres et al. 2015a). Data were visualized via multi-variate homogeneity of group dispersions using the `betadisper` function from the `vegan` package (Oksanen et al. 2013) in R. Finally, group dissimilarity in venom expression was estimated using Euclidean distances in the `dist` and `meandist` functions in R as previously described (Margres et al. 2019).

Venom-gland RNA-seq Library Preparation, Sequencing, and Processing

We sequenced venom-gland transcriptomes for two island adult *C. adamanteus* and downloaded 12 publicly available *C. adamanteus* venom-gland transcriptomes from NCBI SRA (PRJNA88989; Table S1; Rokyta et al. 2017; Hogan et al. 2024); the complete dataset contained mainland juveniles ($n = 6$), mainland adults

($n = 4$), island juveniles ($n = 1$), and island adults ($n = 3$). For each individual, venom was extracted four days prior to euthanasia to allow maximum transcription upon venom gland extraction (Rotenberg et al. 1971). At four days, snakes were euthanized and dissected, and left and right venom glands were placed in RNALater. We extracted RNA from the left and right venom glands separately using the TRIzol extraction method outlined in Rokyta et al. (2017). We sequenced left and right venom glands independently except for one mainland juvenile for which glands were combined prior to sequencing (Table S1) as previously described (Hogan et al. 2024); right and left glands have been shown to exhibit nearly identical expression profiles Rokyta et al. (2015). RNA libraries were generated using the NEBNext Ultra II RNA Library Prep Kit for Illumina (New England Biolabs) following the NEBNext Poly(A) mRNA Magnetic Isolation Module and sequenced at the Florida State University DNA Sequencing Facility on a NovaSeq 6000 with 150 paired-end sequencing. The number of read pairs per library ranged from 1,861,314 to 25,668,566 (Table S3).

We trimmed all reads using Trim Galore! with default parameters (Krueger 2015) and assessed read quality with FastQC (Leggett et al. 2013). We used Hisat2 (Kim et al. 2019) with parameters `-k 10` and `-dta` to map each transcriptome to the reference genome *Cadamanteus_3dDNAHiC_1.2* (Hogan et al. 2024). For all individuals except for the single mainland juvenile described above, mapped left and right venom gland transcriptomes were merged using `samtools merge` (Danecek et al. 2021). We then estimated read counts for genes using HTSeq-count with `-minqual 10` (Anders et al. 2015; Putri et al. 2022) to remove reads with >10% probability of multiple alignments, and calculated transcript-per-million (TPM) of each gene using Stringtie2 (Pertea et al. 2015).

Characterizing Venom-gland Transcriptome Expression Differentiation

To identify specific venom genes and TFs that were DE across populations and/or age classes, we used DESeq2 (Love et al. 2014) on raw, unnormalized counts from our venom-gland transcriptome data ($n = 14$). We conducted all six pairwise comparisons across the four groups: mainland juveniles ($n = 6$), mainland adults ($n = 4$), island juveniles ($n = 1$), and island adults ($n = 3$); significance in differential expression was calculated using the false-discovery rate (FDR)-adjusted p -value and $LFC \geq 1$. We recognize that $LFC \geq 2$ is more often used for identifying DE transcripts, but given (1) that we were confirming and investigating at greater resolution the expression differentiation identified in

our larger proteomic data set ($n = 46$) and previous work (Margres et al. 2017), and (2) our relatively small RNA-seq sample sizes (particularly with a single island juvenile), we elected to use a less stringent cut-off. To visualize the differential expression results, a volcano plot was created using the EnhancedVolcano package in R (v1.24; Blighe et al. 2024). To assess the degree of nucleotide similarity among paralogous SVSP toxin genes in the reference genome, we first extracted coding sequences (CDS) for each gene family using gffread (Pertea and Pertea 2020) with the -x flag. Pairwise nucleotide alignments were performed using EMBOSS: needleall with a gap opening penalty of 10 and a gap extension penalty of 0.5. Pairwise percent identities were parsed from the alignment output and summarized across all gene pairs for each family.

For DE TFs, GO terms were assigned to protein sequences using InterProScan (v5.72-103.0; Jones et al. 2014). GO annotations were extracted from the InterProScan results, and redundant rows and invalid entries were removed to create a cleaned GO annotation dataset. GO enrichment analysis was conducted using the clusterProfiler package in R (v4.14.4; Wu et al. 2021). The enricher function was applied to identify overrepresented GO terms in the DE TF list relative to a background set of all TFs. The input consisted of a list of DE TFs from the venom gland dataset, background genes containing all TFs with associated GO terms actively expressed in the venom glands, and a two-column data frame mapping GO terms to corresponding gene IDs. Enrichment was assessed using the hypergeometric test, with FDR-adjusted p -values. GO terms with FDR values < 0.05 were considered significantly enriched.

ATAC-seq Library Preparation, Sequencing, and Processing

We performed venom-gland ATAC-seq for two island adult individuals and downloaded venom-gland ATAC-seq data for six additional mainland individuals (PRJNA868880; Table S1; Hogan et al. 2024); the complete dataset contained mainland juveniles ($n = 4$), mainland adults ($n = 2$), and island adults ($n = 2$). We also conducted ATAC-seq on liver, muscle, and spleen for one island adult (MM0372; Table S1). ATAC-seq was conducted following the Omni-ATAC-seq protocol (Corces et al. 2017) with modifications outlined in Hogan et al. (2024). Briefly, we collected tissue from freshly dissected venom-glands, liver, muscle, and spleen and proceeded immediately to nuclei isolation and library preparation. We sheared 30 – 100 mg of tissue and washed with ice-cold phosphate-buffered saline. Samples were then resuspended in ice-cold ATAC-resuspension buffer (10 mM Tris-HCL, 10 mM NaCl, 3 mM MgCl₂, 0.01%

digitonin, 0.1% Tween-20, and 0.1% NP40), and nuclei were extracted (Corces et al. 2017). We counted nuclei using hemocytometer chips, and ~ 50, 000 to 60, 000 intact nuclei were transposed using the Illumina Tagment DNA TDE1 Enzyme and Buffer Kit. We then cleaned the reaction using a Zymo DNA Clean and Concentrator-5 kit. Transposed DNA was PCR amplified for five to six cycles. We used qPCR to determine the number of PCR cycles needed for effective amplification of each sample without oversaturation. The PCR amplified libraries were then purified with Agencourt AMPure XP beads (Beckman Coulter). We used KAPA PCR to determine amplifiable concentrations and sequenced the libraries on an Illumina NovaSeq 6000 at the Florida State University DNA Sequencing Facility. The number of read pairs per library ranged from 10,691,848 to 110,972,116 (Table S3).

We trimmed ATAC-seq reads using Trim Galore! v0.4.4 (Krueger and Andrews 2011) using -quality 23 and all other parameters at default. Read quality was assessed with FastQC (Leggett et al. 2013). We used Bowtie2 v2.4.2 (Langmead and Salzberg 2012) at default settings to align the trimmed reads to the reference genome *Cadomantemus_3dDNAHIC_1.2* (Hogan et al. 2024) and removed all reads aligning to mitochondrial DNA. We then used Picard MarkDuplicates v2.25.4 to remove optical and PCR duplicate reads and merged reads from the left and right venom glands with Samtools merge. Next, we called ATAC-seq peaks with MACS2 version 2.2.6 (Zhang et al. 2008) with a p -value cutoff of 0.01 on the aligned BAM files. To identify venom-specific regions of accessibility, peaks within venom glands that overlapped with a control, non-venom tissue (i.e. liver, muscle, or spleen) were removed with bedtools subtract with the following parameters: -A, -f 0.50, and -r; such an approach removed entire venom peaks reciprocally overlapping with control peaks by at least 50% as previously described (Margres et al. 2021a).

Estimating Differential Chromatin Accessibility in Venom Genes

Using the ATAC-seq data, we determined the DA of venom genes in venom glands between mainland juveniles ($n = 4$), mainland adults ($n = 2$), and island adults ($n = 2$). For each of the samples, only venom-specific ATAC-seq peaks within 10 kb of a venom gene were retained. We then classified the remaining peaks based on proximity to the closest venom gene as 10 kb upstream/downstream, 1 kb upstream/downstream, or within the venom gene, consistent with previous work (Hogan et al. 2024). Any peak overlapping two categories was classified based on the closer categorization (e.g. a peak overlapping 10 kb upstream/downstream and 1

kb upstream/downstream was considered 1 kb upstream/downstream). We then counted reads within the identified venom peaks with HT-seq count, using the venom peak file generated for each sample as a reference to ensure read counts were generated only for accessible genomic regions (i.e. those possessing a peak) within or nearby an annotated venom gene. We ran HT-seq count under the following four filtering schemes: `-nonunique=none`, `-minqual=10` and `-nonunique=all`, `-minqual=0, 10`, or `20`. `-nonunique=all` retains reads overlapping multiple regions whereas `-nonunique=none` removes such reads. For example, if a peak overlapped with both a 1 kb and 10 kb region upstream from a venom gene, a read within the peak may overlap both regions. `-nonunique=all` would increase the count of both regions for such an overlapping read, and `-nonunique=none` would not count the read. Because venom peaks often overlapped with two venom regions, most of our filters retained reads overlapping multiple regions (i.e. `-nonunique=all`). To determine the overall accessibility of a genic region, we summed all venom peak read counts within each genic region (e.g. within a 10 kb upstream region) and then summed counts across equivalent upstream and downstream regions (e.g. 10 kb upstream and 10 kb downstream). To identify DA of specific venom ATAC-seq peaks and venom genes, we used DESeq2 (Love et al. 2014) as previously described (Hogan et al. 2024). Due to the low number of replicates ($n = 2$ each for island and mainland adults), we considered a region DA if it had a LFC ≥ 1 . Venom genes were considered DA if they had (1) at least one region with LFC ≥ 1 across more than one filter and (2) no conflicting bias (e.g. a single region was island biased under one filter but mainland biased under another, or an upstream region was island biased but a downstream region was mainland biased would be removed).

Exploring Sequence Variation in Chromatin Accessible Venom Regions

To determine if sequence variation was present in ATAC-seq peak regions within and flanking venom genes, we called SNPs on the aligned, de-duplicated reads (see above). We followed the GATK pipeline (version 4.2.0.0; Poplin et al. 2018), first using HaplotypeCaller with the `"-ERC GVCF"` and `"-do-not-run-physical-phasing"` flags on each sample. To generate jointly genotyped SNPs and indels, we combined sample-level SNP calls with GenomicsDBImport and used GenotypeGVCFs to extract variants. We next used SelectVariants to obtain only SNPs and ran VariantFiltration with filters `QD < 2.0`, `FS > 60.0`, `MQ < 40.0`, `MQRanksSum < -12.5`, and `ReadPosRankSum < 8.0` as recommended by GATK

developers. Finally, we used VCFtools (Danecek et al. 2011) to retain SNPs found within ATAC-seq peaks. We further filtered this final set of SNPs by (1) separating island from mainland snakes, (2) using `-minGQ 5` (i.e. probability of an incorrect genotype call $< 10\%$), and (3) removing variants where fewer than two island or mainland snakes possessed genotypes.

Identifying Structural Variants through BioNano Optical Mapping

To identify large SVs (i.e. > 500 bp) in the island population compared to the mainland population, we used Bionano optical mapping. A single blood sample from an island adult (KW1729; Table S1) was sent to Bionano Genomics (San Diego, CA) where high-molecular weight DNA was extracted, fluorescently-tagged with DLE1 (i.e. CTAAAG motifs), and imaged on a Saphyr system resulting in > 12 million optically mapped molecules. After filtering (molecules ≥ 150 kbp with ≥ 9 labeled sites), a total of 1.49 Tbp of DNA (N50 of 294.38 kbp) resulted in $\sim 928\times$ optical mapping genome coverage.

Data were processed using Bionano Solves (v3.7) Rare Variant Analysis (RVA) pipeline. The RVA pipeline detects SVs via "split-read" and copy-number variant analyses. The "split-read" analysis identifies SVs by analyzing molecule alignments and looking for clusters of molecules with internal alignment gaps and multiple alignments. The copy number analysis detects SVs by finding regions of the genome with significantly increased or decreased coverage. See here for details: <https://bionanogenomics.com/wp-content/uploads/2018/04/30110-Bionano-Solve-Theory-of-Operation-Structural-Variant-Calling.pdf>.

Supplementary Material

Supplementary material is available at *Genome Biology and Evolution* online.

Acknowledgments

The authors thank Nathanael Herrera, Pierson Hill, Flavio Morrissiey, Joe Pfaller, Micaiah Ward, and Tucker Heptinstall for their assistance in the field. The authors thank Megan Lamb, Danielle Jones, Ethan Bourque, Jennifer Wanat, Rebecca Bernard, Caitlin Snyder, and Lexington Preheim with the Florida DEP and Apalachicola River NERR for access to field sites.

Funding

This work was supported by the National Science Foundation (DEB 1145978 to D.R.R.), the Gopher

Tortoise Council (to M.J.M.), Florida State University (to D.R.R. and M.J.M.), and the University of South Florida (to M.J.M.).

Conflict of Interest

The authors declare no competing interests.

Data Availability

Morphological and raw proteomic data are provided in [Tables S1](#) and [S2](#), respectively. Reads were deposited in the NCBI Sequence Read Archive under BioProject PRJNA1244553 and accessions SRR32929610–23. Bionano data are available under accession SUPPF_0000005669. Scripts used for venom-gland RNA-Seq processing and expression differentiation analyses are available here: https://github.com/SamuelRHirst/Manuscript_Code/tree/main/Truncated_Life_History_Evolution_Margres_2026. Scripts used for venom-gland ATAC-Seq processing and the differential accessibility analysis are available here: https://github.com/D-gallinson/Truncated_Life_History_Evolution_Margres_2026_ATAC_seq.

Literature cited

- Anders S, Pyl PT, Huber W. HTSeq—a Python framework to work with high-throughput sequencing data. *Bioinformatics*. 2015;31:166–169. <https://doi.org/10.1093/bioinformatics/btu638>.
- Barrett RDH, Rogers SM, Schluter D. Natural selection on a major armor gene in threespine stickleback. *Science*. 2008;322:255–257. <https://doi.org/10.1126/science.1159978>.
- Barrett RDH, Schluter D. Adaptation from standing genetic variation. *Trends Ecol Evol*. 2007;23:38–44. <https://doi.org/10.1016/j.tree.2007.09.008>.
- Beerli P. Migrate version 3.0: a maximum likelihood and Bayesian estimator of gene flow using the coalescent. On line, 2008. Current version available at <http://popgen.sc.fsu.edu/Migrate/Migrate-n.html>.
- Blighe K, Rana S, Lewis M. EnhancedVolcano: Publication-ready volcano plots with enhanced colouring and labeling. 2024. Available from: <https://github.com/kevinblighe/EnhancedVolcano>.
- Boback SM, Guyer C. Empirical evidence for an optimal body size in snakes. *Evolution*. 2003;57:345–451. <https://doi.org/10.1111/j.0014-3820.2003.tb00268.x>.
- Borja M et al. Venom variation and ontogenetic changes in the *Crotalus molossus* complex: insights into composition, activities, and antivenom neutralization. *Comp Biochem Phys C*. 2025;290:110129. <https://doi.org/10.1016/j.cbpc.2025.110129>.
- Calvete JJ et al. Snake venomomics of the Central American rattlesnake *Crotalus simus* and the South American *Crotalus durissus* complex points to neurotoxicity as an adaptive paedomorphic trend along *Crotalus* dispersal in South America. *J Prot Res*. 2010;9:528–544. <https://doi.org/10.1021/pr9008749>.
- Cameron DL, Tu AT. Chemical and functional homology of myotoxin A from prairie rattlesnake venom and crotamine from South American rattlesnake venom. *Biochim Biophys Acta*. 1978;532:147–154. [https://doi.org/10.1016/0005-2795\(78\)90457-9](https://doi.org/10.1016/0005-2795(78)90457-9).
- Carroll SP, Hendry AP, Reznick DN, Fox CW. Evolution on ecological time-scales. *Funct Ecol*. 2007;21:387–393. <https://doi.org/10.1111/j.1365-2435.2007.01289.x>.
- Case TJ. A general explanation for insular body size trends in terrestrial vertebrates. *Ecology*. 1978;59:1–18. <https://doi.org/10.2307/1936628>.
- Casewell NR, Wagstaff SC, Harrison RA, Renjifo C, Wüster W. Domain loss facilitates accelerated evolution and neofunctionalization of duplicate snake venom metalloproteinase toxin genes. *Mol Biol Evol*. 2011;28:2637–2649. <https://doi.org/10.1093/molbev/msr091>.
- Corces MR et al. An improved ATAC-seq protocol reduces background and enables interrogation of frozen tissues. *Nat Methods*. 2017;14:959–962. <https://doi.org/10.1038/nmeth.4396>.
- Danecek P et al. The variant call format and VCFtools. *Bioinformatics*. 2011;27:2156–2158. <https://doi.org/10.1093/bioinformatics/btr330>.
- Danecek P et al. Twelve years of samtools and bcftools. *Gigascience*. 2021;10:giab008. <https://doi.org/10.1093/gigascience/giab008>.
- Das A et al. Bayesian integration of genetics and epigenetics detects causal regulatory SNPs underlying expression variability. *Nat Commun*. 2015;6:1–11. <https://doi.org/10.1038/ncomms9555>.
- Di-Poi N et al. Changes in Hox genes' structure and function during the evolution of the squamate body plan. *Nature*. 2010;464:99–103. <https://doi.org/10.1038/nature08789>.
- Donohue K. Why ontogeny matters during adaptation: developmental niche construction and pleiotropy across the life cycle in *Arabidopsis thaliana*. *Evolution*. 2013;68:32–47. <https://doi.org/10.1111/evo.12284>.
- Durban J et al. Integrated “omics” profiling indicates that miRNAs are modulators of the ontogenetic venom composition shift in the Central American rattlesnake, *Crotalus simus simus*. *BMC Genomics*. 2013;14:1–17. <https://doi.org/10.1186/1471-2164-14-1>.
- Egozcue JJ, Pawlowsky-Glahn V, Mateu-Figueras G, Barceló-Vidal C. Isometric logratio transformations for compositional data analysis. *Math Geol*. 2003;35:279–300. <https://doi.org/10.1023/A:1023818214614>.
- Erdoğan DE et al. ATAC-seq in emerging model organisms: challenges and strategies. *J Exp Zool Part B*. 2025. <https://doi.org/10.1002/jez.b.23305>.
- Fang B, Edwards SV. Fitness consequences of structural variation inferred from a house finch pangenome. *Proc Natl Acad Sci U S A*. 2024;121:e2409943121. <https://doi.org/10.1073/pnas.2409943121>.
- Forsman A. Variation in sexual size dimorphism and maximum body size among adder populations: effects of prey size. *J Anim Ecol*. 1991;60:253–267. <https://doi.org/10.2307/5458>.
- Forsman A, Lindell LE. The advantage of a big head: swallowing performance in adders, *Vipera berus*. *Funct Ecol*. 1993;7:183–189. <https://doi.org/10.2307/2389885>.
- Foster JB. Evolution of mammals on islands. *Nature*. 1964;202:234–235. <https://doi.org/10.1038/202234a0>.
- Foucher I et al. Hoxa5 overexpression correlates with IGFBP1 upregulation and postnatal dwarfism: evidence for an interaction between Hoxa5 and Forkhead box transcription factors. *Development*. 2002;129:4065–4074. <https://doi.org/10.1242/dev.129.17.4065>.
- Gibbons JW. Reproduction, growth, and sexual dimorphism in the Canebrake Rattlesnake (*Crotalus horridus atricaudatus*).

- Copeia. 1972:1972:222–226. <https://doi.org/10.2307/1442480>.
- Gibbs HL, Sanz L, Calvete JJ. Snake population venomomics: proteomics-based analyses of individual variation reveals significant gene regulation effects on venom protein expression in *Sistrurus rattlesnakes*. *J Mol Evol*. 2009;68:113–125. <https://doi.org/10.1007/s00239-008-9186-1>.
- Gopalan SS et al. Diverse gene regulatory mechanisms alter rattlesnake venom gene expression at fine evolutionary scales. *Genome Biol Evol*. 2024;16:evae110. <https://doi.org/10.1093/gbe/evae110>.
- Greene HW, Wiseman KD. Heavy, bulky, or both: what does “large prey” mean to snakes? *J Herpetol*. 2023;57:340–366. <https://doi.org/10.1670/22-068>.
- GTEx Consortium. Genetic effects on gene expression across human tissues. *Nature*. 2017;550:204–213. <https://doi.org/10.1038/nature24277>.
- Guedouar EG, Hirst SR, Solis SS, Chaput D, Margres MJ. Ontogenetic co-option of myotoxin expression variation in island eastern diamondback rattlesnake (*Crotalus adamanteus*) venoms. *Toxicon*. 2026;277:109094. <https://doi.org/10.1016/j.toxicon.2026.109094>.
- Halfon M. Perspectives on gene regulatory network evolution. *Trends Genet*. 2017;33:436–447. <https://doi.org/10.1016/j.tig.2017.04.005>.
- Hampton PM. Ontogenetic prey size selection in snakes: predator size and functional limitations to handling minimum prey sizes. *Zoology*. 2018;126:103–109. <https://doi.org/10.1016/j.zool.2017.11.006>.
- Harris RB, Sackman A, Jensen JD. On the unfounded enthusiasm for soft selective sweeps ii: examining recent evidence from humans, flies, and viruses. *PLoS Genet*. 2018;14:e1007859. <https://doi.org/10.1371/journal.pgen.1007859>.
- Head JJ, Polly PD. Evolution of the snake body form reveals homoplasy in amniote Hox gene function. *Nature*. 2015;520:86–89. <https://doi.org/10.1038/nature14042>.
- Hirst SR et al. Where the ‘ruber’ meets the road: using the genome of the red diamond rattlesnake to unravel the evolutionary processes driving venom evolution. *Genome Biol Evol*. 2024;16:evae198. <https://doi.org/10.1093/gbe/evae198>.
- Hirst SR et al. Island biogeography and competition drive rapid venom complexity evolution across rattlesnakes. *Evolution*. 2025;79:qpaf074. <https://doi.org/10.1093/evolut/qpaf074>.
- Hirst SR et al. Lack of an ontogenetic shift in *Crotalus enyo* ceral-venis venom supports integration of cranial morphology and venom expression in rattlesnakes. *West N Am Nat*. 2026;86:76–86.
- Hogan M et al. The genetic regulatory architecture and epigenomic basis for age-related changes in rattlesnake venom. *P Natl Acad Sci USA*. 2024;121:e2313440121. <https://doi.org/10.1073/pnas.2313440121>.
- Innan H, Kim Y. Pattern of polymorphism after strong artificial selection in a domestication event. *Proceedings of the National Academy of Sciences*. 2004;101:10667–10672. <https://doi.org/10.1073/pnas.0401720101>.
- Iverson JB. Notes on the natural history of the Caicos Islands Dwarf Boa, *Tropidophis greenwayi*. *Caribb J Sci*. 1986;22:191–198.
- Jensen JD. On the unfounded enthusiasm for soft selective sweeps. *Nat Commun*. 2014;5:5281. <https://doi.org/10.1038/ncomms6281>.
- Jones P et al. Interproscan 5: genome-scale protein function classification. *Bioinformatics*. 2014;30:1236–1240. <https://doi.org/10.1093/bioinformatics/btu031>.
- Kawajiri M et al. Ontogenetic stage-specific quantitative trait loci contribute to divergence in developmental trajectories of sexually dimorphic fins between medaka populations. *Mol Ecol*. 2014;23:5258–5275. <https://doi.org/10.1111/mec.12933>.
- Keehn J, Nieto N, Tracy C, Gienger C, Feldman C. Evolution on a desert island: body size divergence between the reptiles of Nevada’s Anaho Island and the mainland around Pyramid Lake. *J Zool*. 2013;291:269–278. <https://doi.org/10.1111/jzo.12066>.
- Keogh JS, Scott IA, Hayes C. Rapid and repeated origin of insular gigantism and dwarfism in Australian tiger snakes. *Evolution*. 2005;59:226–233. <https://doi.org/10.1111/j.0014-3820.2005.tb00909.x>.
- Kim B et al. Antarctic blackfin icefish genome reveals adaptations to extreme environments. *Nat Ecol Evol*. 2019;3:469–478. <https://doi.org/10.1038/s41559-019-0812-7>.
- Krueger F. TrimGalore!: a wrapper around Cutadapt and FastQC to consistently apply adapter and quality trimming to FastQ files, with extra functionality for RRBS data. Babraham Institute. 2015.
- Krueger F, Andrews S. Bismark: a flexible aligner and methylation caller for Bisulfite-seq applications. *Bioinformatics*. 2011;27:1571–1572. <https://doi.org/10.1093/bioinformatics/btr167>.
- Krumlauf R. Hox genes in vertebrate development. *Cell*. 1994;78:191–201. [https://doi.org/10.1016/0092-8674\(94\)90290-9](https://doi.org/10.1016/0092-8674(94)90290-9).
- Langmead B, Salzberg SL. Fast gapped-read alignment with Bowtie 2. *Nat Methods*. 2012;9:357–359. <https://doi.org/10.1038/nmeth.1923>.
- Leggett RM, Ramirez-Gonzalez RH, Clavijo BJ, Waite D, Davey RP. Sequencing quality assessment tools to enable data-driven informatics for high throughput genomics. *Front Genet*. 2013;4:288. <https://doi.org/10.3389/fgene.2013.00288>.
- Lewis J, Reed R. Genome-wide regulatory adaptation shapes population-level genomic landscapes in *Heliconius*. *Mol Biol Evol*. 2018;36:159–173. <https://doi.org/10.1093/molbev/msy209>.
- Lillywhite H, Martins M. Islands and snakes: isolation and adaptive evolution. Oxford University Press; 2019.
- Lomolino MV. Body size evolution in insular vertebrates: generality of the island rule. *J Biogeogr*. 2005;32:1683–1699. <https://doi.org/10.1111/j.1365-2699.2005.01314.x>.
- Losos J, Warheitt K, Schoener T. Adaptive differentiation following experimental island colonization in *Anolis* lizards. *Nature*. 1997;387:70–73. <https://doi.org/10.1038/387070a0>.
- Losos JB, Ricklefs RE. Adaptation and diversification on islands. *Nature*. 2009;457:830–836. <https://doi.org/10.1038/nature07893>.
- Love M, Huber W, Anders S. Moderated estimation of fold change and dispersion for RNA-seq data with DESeq2. *Genome Biol*. 2014;15:550. <https://doi.org/10.1186/s13059-014-0550-8>.
- Mackessy SP. Venom ontogeny in the Pacific rattlesnakes *Crotalus viridis helleri* and *C. v. oregonus*. *Copeia*. 1988;1988:92–101. <https://doi.org/10.2307/1445927>.
- Mackessy SP. Evolutionary trends in venom composition in the Western Rattlesnakes (*Crotalus viridis* sensu lato): toxicity vs. tenderizers. *Toxicon*. 2010;55:1463–1474. <https://doi.org/10.1016/j.toxicon.2010.02.028>.
- Mackessy SP, Saviola AJ. Understanding biological roles of venoms among the caenophidia: The importance of rear-fanged snakes, 2016.
- Mackessy SP, Williams K, Ashton KG. Ontogenetic variation in venom composition and diet of *Crotalus oregonus concolor*: a case of venom paedomorphosis? *Copeia*. 2003;2003:769–782. <https://doi.org/10.1643/HA03-037.1>.
- Mallo M. Reassessing the role of Hox genes during vertebrate development and evolution. *Trends Genet*. 2018;34:209–217. <https://doi.org/10.1016/j.tig.2017.11.007>.

- Mallo M, Alonso CR. The regulation of Hox gene expression during animal development. *Development*. 2013;140:3951–3963. <https://doi.org/10.1242/dev.068346>.
- Margres M et al. Linking the transcriptome and proteome to characterize the venom of the eastern diamondback rattlesnake (*Crotalus adamanteus*). *J Proteomics*. 2014;96:145–158. <https://doi.org/10.1016/j.jprot.2013.11.001>.
- Margres M et al. Contrasting modes and tempos of venom expression evolution in two snake species. *Genetics*. 2015a;199:165–176. <https://doi.org/10.1534/genetics.114.172437>.
- Margres M et al. Phenotypic integration in the feeding system of the eastern diamondback rattlesnake (*Crotalus adamanteus*). *Mol Ecol*. 2015b;24:3405–3420. <https://doi.org/10.1111/mec.13240>.
- Margres M et al. Expression differentiation is constrained to low-expression proteins over ecological timescales. *Genetics*. 2016a;202:273–283. <https://doi.org/10.1534/genetics.115.180547>.
- Margres M et al. Functional characterizations of venom phenotypes in the eastern diamondback rattlesnake (*Crotalus adamanteus*) and evidence for expression-driven divergence in toxic activities among populations. *Toxicon*. 2016b;119:28–38. <https://doi.org/10.1016/j.toxicon.2016.05.005>.
- Margres M et al. Quantity, not quality: rapid adaptation in a polygenic trait proceeded exclusively through expression differentiation. *Mol Biol Evol*. 2017;34:3099–3110. <https://doi.org/10.1093/molbev/msx231>.
- Margres M et al. Tipping the scales: the migration-selection balance leans toward selection in snake venoms. *Mol Biol Evol*. 2019;36:271–282. <https://doi.org/10.1093/molbev/msy207>.
- Margres M, Bigelow A, Lemmon E, Lemmon A, Rokyta D. Selection to increase expression, not sequence diversity, precedes gene family origin and expansion in rattlesnake venom. *Genetics*. 2017;206:1569–1580. <https://doi.org/10.1534/genetics.117.202655>.
- Margres MJ et al. The Tiger Rattlesnake genome reveals a complex genotype underlying a simple venom phenotype. *Proc Natl Acad Sci U S A*. 2021a;118:e2014634118. <https://doi.org/10.1073/pnas.2014634118>.
- Margres MJ et al. Varying intensities of introgression obscure incipient venom-associated speciation in the timber rattlesnake (*Crotalus horridus*). *Toxins (Basel)*. 2021b;13:782. <https://doi.org/10.3390/toxins13110782>.
- Margres MJ et al. Varying intensities of introgression obscure incipient venom-associated speciation in the timber rattlesnake (*Crotalus horridus*). *Toxins (Basel)*. 2021c;13:782. <https://doi.org/10.3390/toxins13110782>.
- Martín-del Campo R, Sifuentes-Romero I, García-Gasca A. Hox genes in reptile development, epigenetic regulation, and teratogenesis. *Cytogenet Genome Res*. 2019;157:34–45. <https://doi.org/10.1159/000495712>.
- Martin-Fernandez J, Barcelo-Vidal C, Pawlowsky-Glahn V. Dealing with zeros and missing values in compositional data sets using nonparametric imputation. *Math Geol*. 2003;35:253–278. <https://doi.org/10.1023/A:1023866030544>.
- Means D. *Diamonds in the rough, natural history of the eastern diamondback rattlesnake*. Tall Timbers Press; 2017.
- Messer PW, Petrov DA. Population genomics of rapid adaptation by soft selective sweeps. *Trends Ecol Evol*. 2013;28:659–669. <https://doi.org/10.1016/j.tree.2013.08.003>.
- Millien V. Morphological evolution is accelerated among island mammals. *PLoS Biol*. 2006;4:e321. <https://doi.org/10.1371/journal.pbio.0040321>.
- Nachtigall PG et al. A segregating structural variant defines novel venom phenotypes in the eastern diamondback rattlesnake. *Mol Biol Evol*. 2025;42:msaf058. <https://doi.org/10.1093/molbev/msaf058>.
- Oksanen J et al. Package ‘vegan’. *Community ecology package, version, 2(9)*: 1-295.
- Orr HA. The genetics of species differences. *Trends Ecol Evol*. 2001;16:343–350. [https://doi.org/10.1016/s0169-5347\(01\)02167-x](https://doi.org/10.1016/s0169-5347(01)02167-x).
- Osada N, Miyagi R, Takahashi A. *Cis-* and *trans-*regulatory effects on gene expression in a natural population of *Drosophila melanogaster*. *Genetics*. 2017;206:2139–2148. <https://doi.org/10.1534/genetics.117.201459>.
- Perry BW et al. Snake venom gene expression is coordinated by novel regulatory architecture and the integration of multiple co-opted vertebrate pathways. *Genome Res*. 2022;32:1058–1073. <https://doi.org/10.1101/gr.276251.121>.
- Pertea G, Pertea M. Gff utilities: gffread and gffcompare. *F1000Res*. 2020;9:304. <https://doi.org/10.12688/f1000research>.
- Pertea M et al. StringTie enables improved reconstruction of a transcriptome from RNA-seq reads. *Nat Biotechnology*. 2015;33:290–295. <https://doi.org/10.1038/nbt.3122>.
- Poplin R et al. 2018. Scaling accurate genetic variant discovery to tens of thousands of samples [preprint]. *bioRxiv*. <https://doi.org/10.1101/201178>.
- Putri GH, Anders S, Pyl PT, Pimanda JE, Zanini F. Analysing high-throughput sequencing data in Python with HTSeq 2.0. *Bioinformatics*. 2022;38:2943–2945. <https://doi.org/10.1093/bioinformatics/btac166>.
- Reznick DN et al. Eco-evolutionary feedbacks predict the time course of rapid life-history evolution. *Am Nat*. 2019;194:671–692. <https://doi.org/10.1086/705380>.
- Rieseberg LH et al. Major ecological transitions in wild sunflowers facilitated by hybridization. *Science*. 2003;301:1211–1216. <https://doi.org/10.1126/science.1086949>.
- Rokyta D, Margres M, Calvin K. Post-transcriptional mechanisms contribute little to phenotypic variation in snake venoms. *G3 (Bethesda)*. 2015;5:2375–2382. <https://doi.org/10.1534/g3.115.020578>.
- Rokyta DR, Margres MJ, Ward MJ, Sanchez EE. The genetics of venom ontogeny in the eastern diamondback rattlesnake (*Crotalus adamanteus*). *PeerJ*. 2017;5:e3249. <https://doi.org/10.7717/peerj.3249>.
- Rotenberg D, Bamberger ES, Kochva E. Studies on ribonucleic acid synthesis in the venom glands of *Vipera palaestinae* (Ophidia, Reptilia). *Biochem J*. 1971;121:609–612. <https://doi.org/10.1042/bj1210609>.
- Rux DR, Wellik DM. Hox genes in the adult skeleton: Novel functions beyond embryonic development. *Dev Dynam*. 2017;246:310–317. <https://doi.org/10.1002/dvdy.24482>.
- Sackton T et al. Convergent regulatory evolution and loss of flight in paleognathous birds. *Science*. 2019;364:74–78. <https://doi.org/10.1126/science.aat7244>.
- Sati S et al. HiCuT: an efficient and low input method to identify protein-directed chromatin interactions. *PLoS Genet*. 2022;18:e1010121. <https://doi.org/10.1371/journal.pgen.1010121>.
- Schendel V, Rash LD, Jenner RA, Undheim EAB. The diversity of venom: the importance of behavior and venom system morphology in understanding its ecology and evolution. *Toxins (Basel)*. 2019;11:666. <https://doi.org/10.3390/toxins11110666>.
- Schild D et al. The origins and evolution of chromosomes, dosage compensation, and mechanisms underlying venom regulation in snakes. *Genome Res*. 2019;29:590–601. <https://doi.org/10.1101/gr.240952.118>.
- Schild DR et al. The roles of balancing selection and recombination in the evolution of rattlesnake venom. *Nat Ecol Evol*.

- 2022;6:1367–1380. <https://doi.org/10.1038/s41559-022-01829-5>.
- Schoenfelder S, Javierre B-M, Furlan-Magaril M, Wingett SW, Fraser P. Promoter capture hi-c: high-resolution, genome-wide profiling of promoter interactions. *J Vis Exp*. 2018;136:57320. <https://doi.org/10.3791/57320>.
- Schonour RB et al. Gradual and discrete ontogenetic shifts in rattlesnake venom composition and assessment of hormonal and ecological correlates. *Toxins (Basel)*. 2020;12:659. <https://doi.org/10.3390/toxins12100659>.
- Shine R. Why do larger snakes eat larger prey items? *Funct Ecol*. 1991;5:493–502. <https://doi.org/10.2307/2389631>.
- Smith CF et al. Snakes on a plain: biotic and abiotic factors determine venom compositional variation in a wide-ranging generalist rattlesnake. *BMC Biol*. 2023;21:136. <https://doi.org/10.1186/s12915-023-01626-x>.
- Strickland J et al. Evidence for divergent patterns of local selection driving venom variation in Mojave Rattlesnakes (*Crotalus scutulatus*). *Sci Rep*. 2018;8:1–15. <https://doi.org/10.1038/s41598-017-17765-5>.
- Surm JM, Moran Y. Insights into how development and life-history dynamics shape the evolution of venom. *Evodevo*. 2021;12:1. <https://doi.org/10.1186/s13227-020-00171-w>.
- Templ M, Hron K, Filzmoser P. robCompositions: an R-package for robust statistical analysis of compositional data. In: *Compositional data analysis. Theory and applications*. John Wiley & Sons; 2011. p. 341–355.
- Vanek JP, Burke RL. Insular dwarfism in female Eastern Hog-nosed Snakes (*Heterodon platirhinos*; Dipsadidae) on a barrier island. *Canadian J Zool*. 2020;98:157–164. <https://doi.org/10.1139/cjz-2019-0137>.
- Van Valen L. Body size and numbers of plants and animals. *Evolution*. 1973;27:27–35. <https://doi.org/10.1111/j.1558-5646.1973.tb05914.x>.
- Voss SR, Shaffer HB. Adaptive evolution via a major gene effect: paedomorphosis in the Mexican axolotl. *P Natl Acad Sci USA*. 1997;94:14185–14189. <https://doi.org/10.1073/pnas.94.25.14185>.
- Waldron JL, Welch SM, Bennett SH, Kalinowsky WG, Mousseau TA. Life history constraints contribute to the vulnerability of a declining North American rattlesnake. *Biol Conserv*. 2013;159:530–538. <https://doi.org/10.1016/j.biocon.2012.11.021>.
- Wang D, Rendon A, Wernisch L. Transcription factor and chromatin features predict genes associated with eQTLs. *Nucleic Acids Res*. 2013;41:1450–1463. <https://doi.org/10.1093/nar/gks1339>.
- Wen X, Lee Y, Luca F, Pique-Regi R. Efficient integrative multi-SNP association analysis via deterministic approximation of posteriors. *Am J Hum Genet*. 2016;98:1114–1129. <https://doi.org/10.1016/j.ajhg.2016.03.029>.
- Wu T et al. clusterprofiler 4.0: a universal enrichment tool for interpreting omics data. *Innovation*. 2021;2:1–10. <https://doi.org/10.1016/j.xinn.2021.100141>.
- Xie B et al. Dynamic genetic differentiation drives the widespread structural and functional convergent evolution of snake venom proteinaceous toxins. *BMC Biol*. 2022;20:4. <https://doi.org/10.1186/s12915-021-01208-9>.
- Xin J et al. Chromatin accessibility landscape and regulatory network of high-altitude hypoxia adaptation. *Nat Commun*. 2020;11:4928. <https://doi.org/10.1038/s41467-020-18638-8>.
- Yan F, Powell D, Curtis D, Wong N. From reads to insight: a hitchhiker's guide to ATAC-seq data analysis. *Genome Biol*. 2020;21:1–16. <https://doi.org/10.1186/s13059-020-1929-3>.
- Yao Q, Rodrigues E, Liu K-b., Snyder C, Culligan N. A Late-Holocene palynological record of coastal ecological change and climate variability from Apalachicola, Florida, USA. *Clim Change Ecol*. 2022;3:100056. <https://doi.org/10.1016/j.ecochg.2022.100056>.
- Zancolli G, Casewell NR. Venom systems as models for studying the origin and regulation of evolutionary novelties. *Mol Biol Evol*. 2020;37:2777–2790. <https://doi.org/10.1093/molbev/msaa133>.
- Zhang L, Reifová R, Halenková Z, Gompert Z. How important are structural variants for speciation? *Genes (Basel)*. 2021;12:1084. <https://doi.org/10.3390/genes12071084>.
- Zhang Y et al. Model-based analysis of ChIP-Seq (MACS). *Genome Biol*. 2008;9:1–9. <https://doi.org/10.1186/gb-2008-9-9-r137>.
- Zuffi MA, Fornasiero S, Picchiotti R, Poli P, Mele M. Adaptive significance of food income in European snakes: body size is related to prey energetics. *Biol J Linn Soc*. 2010;100:307–317. <https://doi.org/10.1111/j.1095-8312.2010.01411.x>.

Associate editor: Matthew Webster